EASA
European Union Aviation Safety Agency

This project has received funding from the European Union's Horizon 2020 Programme

SMART GREEN AND INTEGRATED TRANSPORT

Integrity improvement of rotorcraft main gearbox

D2-8: Final report and conclusions

An Agency of the European Union

Disclaimer

REPORT NUMBER:	D2-8
REPORT CLASSIFICATION:	UNCLASSIFIED
DATE:	21 February 2024
KNOWLEDGE AREA(S):	Research, rotorcraft, MGB components, design limitations, crack prevention
DESCRIPTOR(S):	Component testing, integrated raceway, crack prevention factors, RCF
CUSTOMER:	simulation European Union Aviation Safety Agency
CONTRACT NUMBER:	EASA.2019.C15
OWNER:	European Union Aviation Safety Agency
DISTRIBUTION:	Limited
CLASSIFICATION OF TITLE:	UNCLASSIFIED

Author(s): W. Riesen, S. Hilleke

APPROVED BY:	AUTHOR	REVIEWER	MANAGING DEPARTMENT
Robert Stürzer	Waldemar Riesen Sven Hilleke	Jörg Litzba	AH Tech Drive Train Components

EVALUATE AND DEFINE ROTOR AND ROTOR DRIVE SYSTEM DESIGN OPTIONS TO PREVENT SINGLE POINTS OF CATASTROPHIC FAILURE

Stream 2:

Final report and conclusions

Airbus Helicopters Technik GmbH

Airbus Helicopters Technik GmbH is a worldwide company known for its helicopter transmission systems. With our EASA and FAA privileges we are active for design and development, manufacturing and maintenance of helicopter transmission systems and geared applications for fix wing aircrafts and engines. Our service activities are not only keeping transmission system components airworthy, also mission support for a broad range of customers are conducted. For nearly all helicopter manufacturers around the world, Airbus Helicopters Technik GmbH designs and supplies worldwide turn-key solutions for gearbox and rotor test stands.

Flugplatzstrasse | 34379 Calden, Germany | + 49 5674 701 0 | + 49 5674 701 606 | GIFT-MGB.aviation@zf.com|

SUMMARY

Problem area

The aim of this report is to summarize and draw conclusions on the actions performed within stream 2. The baseline is the contract between EASA and AH Tech (formerly ZFL) [2] according to the EASA tender [1] based on the Horizon 2020 Work Programme Societal Challenge 4 'Smart, green and integrated transport'.

Description of work

Stream 2 of the project deals with the reliability and tolerance to flaws of rotor and rotor drive system gears and bearings when subject to rolling contact fatigue. Wherever possible, typical modes of degradation were evaluated, and the effects of a selected type of flaw on specimens were analyzed, including intrinsic defects and external damage, and the mechanisms involved in the initiation of cracks beginning with these flaws due to rolling contact fatigue. In addition, testing and simulations were conducted to replicate the rolling contact fatigue mechanisms of crack initiation and subsequent propagation.

Results and application

This report presents a summary of all activities carried out during stream 2 of this project. This is accomplished with a summary of tasks according to [1], and deliverables. As a final step, conclusions are presented based on the given tasks, as well as a classification of the results with regard to the scope of the project and future development projects. In addition, some recommendations for future development projects are given, which could extend and support the results derived from this research project.

CONTENTS

ABBREVIATIONS

ACRONYM	DESCRIPTION
2D	Two-dimensional
AH Tech	Airbus Helicopters Technik GmbH
DIN	German Institute for Standardization
EASA	European Union Aviation Safety Agency
FE	Finite Element
FVA	Research Association for Drive Technology
ISO	International Organization for Standardization
MGB	Main gearbox
MVCCI	Modified virtual crack closure integral
RCF	Rolling contact fatigue
SIF	Stress intensity factors
ZF	ZF AG
ZFL	ZF Luftfahrttechnik GmbH

1. Introduction

The aim of this report is to summarize and conclude the actions performed within stream 2, based on the contract between EASA and AH Tech (formerly ZFL) [2] according to the EASA tender [1] based on the Horizon 2020 Work Programme Societal Challenge 4 'Smart, green and integrated transport'.

Stream 2 of the project deals with the reliability and tolerance to flaws of rotor and rotor drive system gears and bearings when subjected to rolling contact fatigue. Wherever possible, typical modes of degradation were evaluated and the effects of a selected type of flaw on specimens were analyzed, including intrinsic defects and external damage and the mechanisms involved in crack initiation beginning with these flaws due to rolling contact fatigue. In addition, testing and simulations were conducted to replicate rolling contact fatigue mechanisms of crack initiation and subsequent propagation.

Chapter 2 Provides a summary of tasks 2, 3, 4, and 5, which are described within the EASA tender [1].

Chapter 3 Describes the actions performed within stream 2 of the project by providing a summary of the deliverable reports D2-1 through D2-7 [3]-[9].

Chapter 4 Provides conclusions of the project associated with the tasks and results, and presents recommendations for further research on this topic.

Table 1 below gives an overview of the deliverables of this research project within stream 2, which will be detailed in the following chapters. The different documents are referenced to specific tasks within the project according to [1].

Document	Title	Task reference	Nature, Scope	Dissemination level
D2-1	Review of the state-of-the-art design criteria for reliability and flaw tolerance in integrated bearing races and list of relevant design parameters identified	2	Report	Public
D2-2	Detailed analysis methodology	2, 3, 4, 5	Report	Public
D2-3	Initial test plan	3, 4, 5	Test plan	Restricted to a group specified by the contracting authority
D2-4	Analysis report and conclusions (design parameters limitations for reliability and flaw tolerance)	2, 3	Report	Restricted to a group specified by the contracting authority
D2-5	Analysis report and conclusions (critical threats and crack development)	4, 5	Report	Restricted to a group specified by the contracting authority
D2-6	Final test plan	3, 4, 5	Test Plan	Restricted to a group specified by the contracting authority
D2-7	Test report and conclusions	3, 4, 5	Report	Public
D2-8	Final report and conclusions	2, 3, 4, 5	Report	Public

Table 1: Overview of deliverables for stream 2

2. Summary of tasks performed within stream 2 according to [1]

2.1 Task 2: Define adequate design parameters for component reliability and tolerance to flaws

Objectives and expected outcomes according to [1]
This task was planned to identify the most significant design parameters for rotor and rotor drive system components with hardened steel bearing races that influence the reliability and tolerance to flaws of these components when subjected to rolling contact fatigue.

The main milestones of this task can be summarized as follows:

- Review of the state of the art available in industry standards, research, and other relevant literature with regard to critical design parameters of gears with integrated bearing races governing their behavior when subjected to rolling contact fatigue
- Identification of the design parameters that play a critical role in ensuring the reliability and flaw tolerance of integrated bearing races when subjected to rolling contact fatigue

The aim of this task is to provide a list of design parameters that are key to controlling the reliability and flaw tolerance of integrated bearing races when subjected to rolling contact fatigue. The role that each of the identified design parameters plays with regard to reliability and flaw tolerance will be understood in general terms in order to allow accurate planning of the analysis and testing activities that will follow in subsequent tasks.

Conclusion
Task 2 of this research project is mainly answered by reports D2-1, D2-2, and D2-4 (see 3 and Table 1).
On the basis of the activities carried out for these deliverables, it was possible to present a list of key parameters that could impact crack propagation behavior. Furthermore, a classification of the parameters according to their criticality and an evaluation of their interaction was performed, which was used to prioritize parameters for implementation within the test campaign of this research project. A general understanding of parameters and basic threats was additionally derived from the first simulations. With this information, it was possible to provide a baseline for further tasks focusing on the main threats presaging crack propagation under rolling contact fatigue.

2.2 Task 3: Develop design parameter limitations

Objectives and expected outcomes according to [1]

Starting from the list of parameters and the body of knowledge developed in the previous task (Task 2), and based on further analysis and testing, plans were made to identify limiting values for these design parameters that would provide acceptable levels of reliability and flaw tolerance for components subject to rolling contact fatigue.

The main milestones of this task can be summarized as follows:

- Evaluation of the impact of parameters (from Task 2) on reliability and flaw tolerance
- Definition of the test plan to gain a deeper understanding of the parameters (for at least 2 race/rolling element material combinations using both nitrided and carburized low alloy steel)

This task is expected to support the derivation of a number of limitations in design parameters that could be used to ensure acceptable levels of reliability and flaw tolerance for hardened races operating under rolling contact fatigue. The limitations aimed to be proposed as part of this task should be technically feasible to implement in rotorcraft gearbox designs.

Conclusion

A pre-selection of parameters was produced based on Task 2 activities; these parameters are ones whose modification in rotorcraft gearbox designs is technically feasible and can be expected to improve crack propagation behavior (see Annex B). To evaluate these parameters, a dedicated test plan (D2-3 and D2-6) was derived with the support of additional simulations (D2-4) on these parameters. As an outcome of the test campaign and the simulations, it was impossible to define clear limits for the given parameters, although the main hypotheses (see D2-2) were substantiated. The limitations of the activities performed for Task 3 (testing) are described in detail in D2-7. Nevertheless, it may be possible to derive specific parameter limitations with the help of further research on this topic (see 4.2).

2.3 Task 4: Determine threats that cannot be addressed by design

Objectives and expected outcomes according to [1]

Based on the analyses and tests from Task 3, a further evaluation was planned to identify the extent of any threats (flaws) that (a) cannot be reliably addressed by design parameters, (b) that have the potential for crack initiation and subsequent propagation through rolling contact fatigue-assisted mechanisms, and (c) that may need additional provisions or mitigation to ensure the safe operation of the system.

The main milestones of this task can be summarized as follows:

- Review of the results of Task 3
- Evaluation of threats that cannot be reliably addressed by means of establishing adequate design parameters but that were identified as capable of supporting flaw tolerance under rolling contact
- Planning and completion of analyses and tests to characterize and specify the consequences of threats that could lead to crack initiation or catastrophic failure of the system

This task is intended to provide a list of threats (and the extent thereof) requiring additional steps to ensure the reliability and flaw tolerance of rotor and rotor drive system components under rolling contact fatigue conditions.

Conclusion

As described above, it was possible to validate the hypothesis (presented within D2-2) thanks to the activities carried out during Task 3 of this project. By proving this hypothesis and evaluating this test campaign, it was also possible to make a clear statement on the objectives of Task 4, i.e. threats that cannot be addressed by design. This is mainly derived from reports D2-4, D2-5 and D2-7.

- The main threats promoting crack propagation are based on the specific design of the component
- A specific combination of residual stress profiles, material properties (fracture-mechanical threshold values) and contact pressure turned out to be the primary drivers of crack propagation in conjunction with the second driver (body stress). This phenomenon is directly linked to the specific design of the component.
- Threats that are typically not directly addressed by the design of the bearing have not been considered as threats as part of this project. These threats could include pre-damage, lubrication issues, or operational conditions that cannot be influenced by the design itself (e.g. temperature).

2.4 Task 5: Investigate crack development in components utilizing hardened materials

Objectives and expected outcomes according to [1]

The objective of this task was to determine the factors that promote crack development back to the surface rather than into the core of a case-hardened/nitrided low-alloy steel component.

The main milestones of this task can be summarized as follows:

- State-of-the-art analysis tools should be used to evaluate the mechanisms of crack propagation.
- Parameters that affect crack propagation should be identified, and their impact on crack growth behavior should be understood and quantified.

The results after completing this task should provide an understanding of the factors that demonstrably impact the crack propagation direction and/or rate due to rolling contact fatigue within rotor and rotor drive system components based on analysis and validated by testing.

Conclusion

The test campaign, as well as the simulations made during the GIFT research project, demonstrated that body stress is the main factor influencing the likelihood of a crack through the material, whereas the other parameters that were simulated and tested within this research project showed a certain influence on crack propagation, but did not lead to a crack through. Therefore, it is necessary to study each case in detail and separately, especially for those cases where additional body stress could not be avoided or where parameters differ significantly from those used within this project. This could be the case for residual stress profiles, which could differ from the values of this research project due to differences in manufacturing steps [9].

3. Summary of activities performed within stream 2 of this research project

3.1 D2-1 [3] and D2-3 [5]

These reports are not detailed here because they are public documents.

3.2 D2-4 [6]: Analysis and conclusion regarding design parameter limitations for reliability and flaw tolerance

The aim of this undertaking was to perform a 2D simulation of crack propagation during rolling contact in parallel to planned testing. For this purpose, the crack loading caused by RCF was analyzed and evaluated in detail for each simulation step of crack propagation. This enabled a better understanding of crack propagation in the structure due to rolling contact fatigue. These simulations were performed using the FE program ABAQUS and the crack propagation simulation program ADAPCRACK3D. The methods developed in this project for investigating crack growth can be applied to other problems of practical relevance, such as rolling contact in planetary gears.

Small defects or cracks due to fatigue crack growth that initially appear harmless can reach a critical length. This can lead to component failure. To assess the safety of a structure, it is important to predict the crack path. If the load, component geometry, and material properties are known, fracture-mechanical stress analysis can be carried out using the finite element method to understand the damage process and predict the crack path in the structure. Due to the large number of mutually interdependent parameters, such as contact geometry, load, lubricating film, rolling velocity, coefficient of friction, material properties, inclusions, microstructure, surface treatment, and impurities, rolling contact fatigue is a complex problem. For the simulation within stream 2, the following important parameters were considered: contact geometry, loading, and friction at the cylinder/half-plane interface and at crack faces. The crack growth simulation was carried out using the stress intensity factor approach with the ADAPCRACK3D program system. Because of the effects of crack closure, crack branching, and the complexity of the applied stress field, there is no perfect method for calculating the stress intensity factors. The calculation of SIFs was performed using the MVCCI method, which uses crack opening displacements of the crack faces near the crack tip and forces on the cross-section before the crack (ligament). Using the σ_1' criterion, the cyclic equivalent SIF ΔK_V as well as the kink angles and the twist angles, are determined. If ΔK_V is smaller than the threshold value, the crack cannot grow. If the crack propagation is stable ($\Delta K_{th} < \Delta K_V < \Delta K_C$), the crack grows by Δa, taking into account the kink angle and twist angle. The aim was to apply the method developed for investigating crack growth to other issues of practical relevance.

The first numerical results were generated in a 2D model and validated with analytical reference solutions. The solutions based on Hertz's theory were used as the reference result. The residual stresses were not accounted for. The analytical and FE results showed good conformance to prominent literature, and these results show that the mesh quality and selected boundary conditions are optimal for FE simulation. Furthermore, stress fields in the half-plane with surface crack when being rolled over were calculated and the curves of the SIFs are determined (Annex C.1) and validated (Annex C.2). A parametric study was also performed to investigate the influence of the crack parameters, friction in the contact areas, and the level of the contact pressure on the crack path. The results showed that shallow crack initiation angles with high contact pressure and low friction at crack faces favor crack branching (Annex C.3), which can lead to spalling.

3.3 D2-5 [7]: Analysis and conclusion on critical threats and crack development

On the basis of the prepared simulation model, the influences of residual stresses and complex load (body stress) on crack development were investigated to underline the testing of Phase I.2 and Phase II.
For this purpose, basic parametric studies were carried out to determine the variables influencing crack angle, crack depth, residual stresses, and complex load. The FE software ABAQUS and the ADAPCRACK3D program for simulating crack propagation were used for these calculations. The crack growth simulation is based on the influences of the Hertzian pressure during rolling contact and the Coulomb friction between the crack flanks. Body stress and residual stress are additional parameters accounted for within the simulations.
The results without considering the complex load (body stress) have shown that the loading parameter K_I for cracks initiated at a shallow angle is increased by the presence of residual stresses after kinking (for details, see [7]). This drives the crack to grow toward the surface, which can result in spalling. In contrast, vertical cracks come to a standstill faster under residual stresses.
The results with a complex load (body stress) have shown that these stresses could cause a failure of the component (Annex D).

The crack propagation simulations were performed to evaluate whether the chosen values are reasonable and if crack propagation might be expected. In such case, checks were performed for propagation only up to a limited depth. The simulations were performed at 1500 MPa and at two additional points (500 MPa and 3000 MPa), without considering residual stress or body stress. These two last contact levels are voluntarily set outside of the defined test range for Phase I to give a broader picture of the influence of contact pressure on the crack propagation path. The simulations were also performed considering different crack angles relative to the surface. For contact pressures of 500 MPa, no crack propagation was observed at all. Differences for contact pressures of 1500 and 3000 MPa were only observed in the mechanical loading and a slight difference was observed in the crack path direction itself. For both cases, crack kinking is possible, depending on the crack starting angle. Nevertheless, all cracks tended to arrest due to the decreasing stress intensity factor.

The limited simulation results currently available, in all scenarios of contact pressure and initial crack angle, predict that the crack propagates and then self-arrests at a limited depth relative to the surface. It was also found that the crack paths differed depending on the initial crack angle and the selected contact pressure.
The simulations indicate that with contact pressures of 1500 MPa as the lower bound and 2400 MPa as the upper bound, crack propagation is expected to stop at a limited depth.

3.4 D2-6 [8]: Final test plan

In the next step, the test specimen and test benches were identified, the type and method of testing to be performed were detailed, and the related inspection and acceptance criteria for verification were determined. Detailed information on the specimens and test benches used is summarized in Annex E In Annex F , there is also an overview table presented, highlighting the different test points that were carried out, including the parameters that were varied.

Phase I.1 of testing focused on the variation in contact pressure, whereas the other parameters were adjusted and fixed according to predefined baseline values. The main procedure and general information about this test Phase are summarized in Figure 1. The definition of the type of defect and size was supported by some pre-tests during Phase I.1, leading to modifications to the initially planned damage to reach the final damage that was used during the entire test campaign.

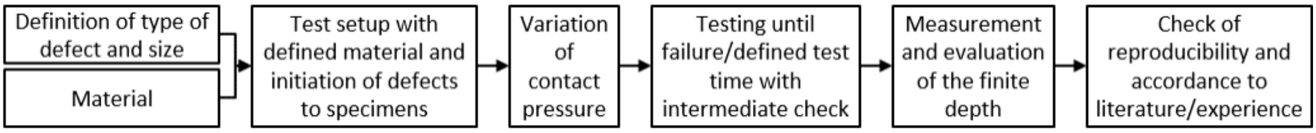

Figure 1: Definition of phase I.1 procedure

Phase I.2 of the test campaign aimed to continue on the two selected test benches with modified specimens. No change was made to the boundary conditions or the introduced pre-damage. The tests were planned for all selected material combinations similar to Phase I.1. The focus for this Phase was on the variation of hardness, residual stress, and hardening depth to evaluate their influence on crack initiation, depth, and shape. The main procedure and general information regarding this test Phase are summarized in Figure 2.

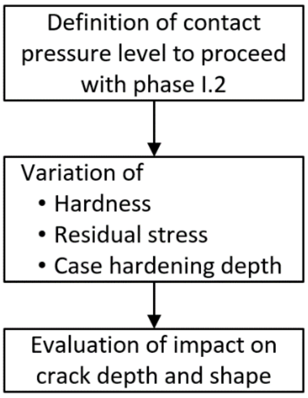

Figure 2: Definition of Phase I.2 procedure

Phase II of testing was focused on the introduction of a complex load situation and the evaluation of its impact on crack propagation. All other parameters remained fixed according to the tested baseline variants from Phase I.1. The main procedure and general information of this test Phase are summarized in Figure 3.

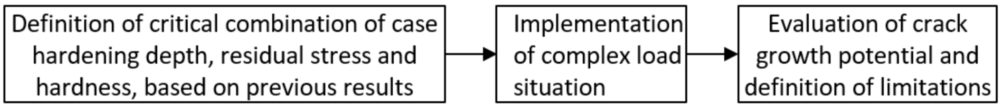

Figure 3: Definition of Phase II procedure

The two different test campaigns were conducted in parallel. The specimens were designed according to the standard configuration used for similar tests at the test benches.

The purpose of the outer ring specimen was to evaluate the integrated outer races. To introduce the complex load situation, the design of the specimen was modified with a notch/groove in the outer ring to enable the outer ring to bend under the roller load (Annex E.1).

The purpose of the shaft specimen was to evaluate integrated inner races. To introduce the complex load situation on this specimen, the solid shaft specimen was replaced by a hollow shaft to enable the application of radial force and therefore a bending load and bending stress on the shaft (Annex E.2).

3.5 D2-7 [9]: Test report and conclusions

The main focus of the work for D2-7 was on the detailed description of test and simulation activities that were done by taking into account the main objectives for tasks 3, 4, and 5 ([1],[2]). This included an evaluation of the tested parameters and an interpretation of all observations made during testing (see also Annex F); also included were a validation and correlation of the simulations performed within the test campaign. The test campaign was divided into three main phases:

- Phase I.1: Pure RCF for different load levels
- Phase I.2: Pure RCF by varying key parameters
- Phase II: RCF with additional body stress (complex load)

These different phases were created in order to validate the hypotheses that were defined and presented in D2-2 [4].
The D2-7 report can be split into two main streams. One stream is evaluation by testing, and the other stream is evaluation and validation by simulation. Various observations were thus obtained for these two streams.

Test campaign

Phase I.1 was used to study the influence of different load levels on the initiation of spalling and cracks under pure RCF for a pre-damaged raceway. The results demonstrated that a limit exists for both materials, below which no spalling could be introduced for the given pre-damage, whereas the load level of 2.4 GPa repeatably produced spalling. Identical observations were made for Phase I.2, where parameters such as hardness depth, hardness, and residual stress were varied. Within the three load levels that were tested, the limit for no spall initiation remained below 2.4 GPa, initiation of spalling was only possible at a load level of 2.4 GPa A more detailed limit could not be identified because only three load levels were tested. Nevertheless, a clear trend for both materials and applications was not observed; it was only the case that specimens with the highest case hardening depth had the lowest spalling depth for the case hardened material. Finally, all the tests for Phase I.1 and I.2 validated the hypothesis that crack growth ends at a finite depth and pure rolling contact typically results in classical spalling damage for the single load condition without further crack growth through the material.
During Phase II, a complex load (second driver) was introduced by modification of the specimens, thereby allowing additional deformations. The tests showed for the outer ring application that the second driver led to severe cracks into the depth of and through the material. It was also shown that for the same load level, no cracks through the material occurred for the nitrided material, which could be explained by a higher crack growth threshold value. For the shaft application, it was only possible at a much higher load level (2.9 GPa) to introduce further crack growth without any crack through the material. Cracks perpendicular to the raceway were observed to be less critical to the bending moment because only the ovalization of the shaft promotes crack propagation as a second driver. Further testing with cracks in the rolling direction should be carried out to prove this hypothesis.
The results, especially with regard to the spalling depth for the shafts from 32CDV13, are only of limited significance, as they did not show any classic spalling. The reason for this is that the white layer is not removed for the nitrided shafts during the manufacturing process and led to a peeling-off of the white layer.

Nevertheless, the test results showed that deeper crack propagation into the depth of the material with a crack through the complete thickness is mainly driven by the second driver (additional body stress), and the potential for this type of failure can be significantly reduced by the reduction or omission of a second driver.

Simulations

Simulations described as part of D2-7 [9] substantiated the statements above. The simulation model developed within the framework of this project validated the test results and the hypothesis that additional body stress is required to promote a crack through the material. In particular, for the outer ring application, it was also possible to predict the crack path with a crack through by considering the present crack initiation based on the maximum spalling depth. The assumption of an initial crack in the simulation is mandatory because the model is based on fracture-mechanical principles, which are not predictive enough to judge spall initiation or crack growth for very small crack lengths.

Nevertheless, the simulations were also capable of showing crack propagation parallel to the surface under specific circumstances depending on the assumptions made (see additional information in [9]).

For the shaft application, some deviations were observed between the simulation and test results, although it must be said that the simulation was based on a number of worst-case load conditions. Nevertheless, the simulation results were always on the conservative side in that they used maximum tensile residual stresses from the measurement/simulation and maximum initial crack length. Moreover, sensitivity analysis (e.g. for crack angle) was performed in order to use the most severe crack condition. The word “conservative” is understood to mean that crack propagation or a crack through is more likely.

Supported by the simulations, it was therefore possible to substantiate the second and third hypotheses given above. The simulation model and its complexity were reduced to 2D and fixed crack growth increments were assumed in order to significantly reduce calculation time for the project. This can be changed, if required, to allow for estimations about 3D cracking or residual lifetime based on da/dN curves (see additional information in [9]).

4. Conclusion and recommendations

4.1 Conclusion

As an overall conclusion within the scope of the project, it is worth mentioning that no fixed limits for the given parameters, load conditions, or body stresses could be presented as generically applicable for other applications. Potential applications could be planetary gears, integrated or non-integrated bearings, gears or integrated raceways on housings, liners, or shafts (this list does not claim to be exhaustive).

The test campaign, as well as the simulations made during the GIFT research project, demonstrated that body stress is the main factor influencing the likelihood of a crack through the material, whereas the other parameters were simulated and tested within this research project showed a certain influence on crack propagation, but these did not lead to a crack through the material. Therefore, each case must be studied separately and in detail, especially for those cases where additional body stress cannot be avoided or where parameters differ significantly from those used within this project. This could be the case for residual stress profiles, which could differ from the values of this research project because of differences in manufacturing steps.

Limits that could be extracted from the test campaign and simulation (e.g., maximum allowable pressure level or body stress) could be different for other applications due to geometrical effects or manufacturing influences (e.g., influence on the crack growth threshold). Nevertheless, it is possible to use the general approach in any other application, taking as a guide the flow chart presented below (see Figure 4).

As a starting point and baseline, four main pillars can be mentioned. These are: the evaluation of the geometry, external load, material properties, and residual stress profile (see Figure 4 for more details on information needed). Moreover, additional information should be derived from available MRO data to ensure that the simulation is conservative. This could be done by additional output of MRO data (e.g., maximum spalling depth or information on subsurface cracks).

A general body of experience on the sensitivity of initial crack depth/angle in response to key parameters is also known thanks to the current research project and could be used in conjunction with the MRO data to build the simulation model properly (e.g. max spalling depth in a range of 0.3-0.5 mm vs. critical crack depth based on residual stress profile for the tested applications). Detailed knowledge on these pillars is mandatory for further evaluation and needs to be done for any new application, which might also lead to the use of further simulation model details (e.g. 2D vs. 3D). Nevertheless, reduced complexity of the model is recommended due to simulation time and could be supported by additional testing. After some sensitivity analysis within the simulation, a statement of potential critical crack growth can be made, which could lead to recommendations for re-design. If critical crack propagation can be ruled out by simulation, additional testing can be used to validate the results and support certification according to CS 27.571/CS 29.571. Additional testing could be necessary for several reasons (see also details in Figure 4).

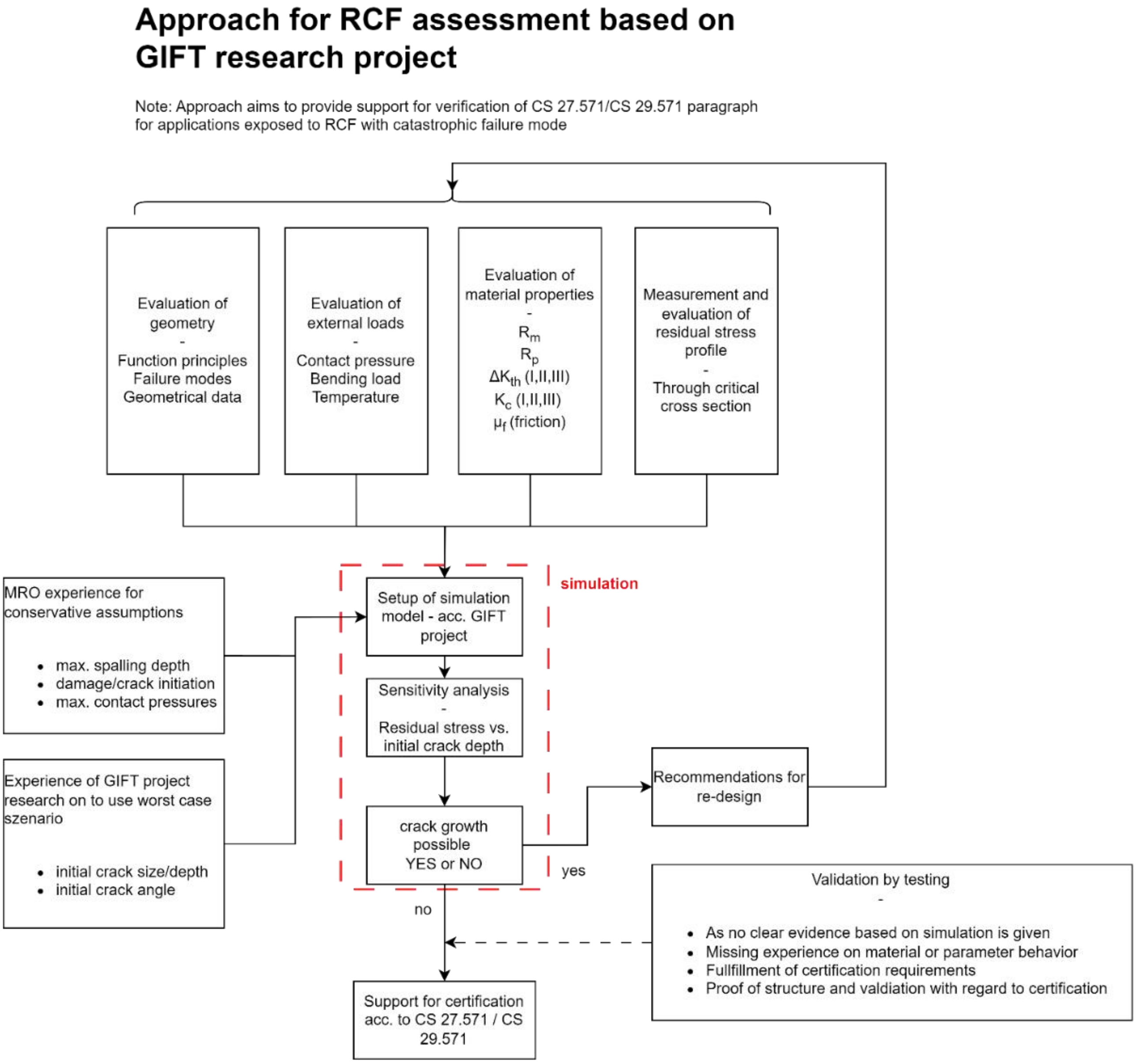

Figure 4: Potential use of experience from this research project within other applications

As shown in Figure 4, the simulations developed and the experience won from testing (see [9]) are not limited to the applications of this research project. They can be transferred to support future development activities and provide recommendations for more sustainable design solutions to avoid critical crack propagation. With the information gained from this research project, it was possible to provide a guideline for future development of components subject to RCF with a catastrophic failure mode.

4.2 Recommendations for further research on this topic

It was not possible to answer in full all initially planned questions based on the activities carried out during this research project. This fact was mainly due to the time constrains of the project and therefore to the limited tests and simulations, as well as the complex interdependencies of the parameters impacting crack propagation behavior as observed during testing and simulation.

To deal with the limited time frame of the project, several compromises and simplifications were necessary. Therefore, the test campaign was limited to two specific types of application with two types of material for each application. The statistically required number of repetitions per version was also reduced to three to significantly reduce the overall testing time. The same reason was also responsible for the use of a single type of defect for all tests (scratch/laser scratch). No further investigations were conducted on other types of defects. There were also a limited number of parameter levels tested (e.g., for contact pressure, residual stress, and body stress level), which was driven by the available test time.

Another point to be mentioned is the fact, that the manufacture-adjusted parameter (hardness, case hardening depth, residual stress) were not fully reached as planned. Differences compared with baseline variant remained small. This was mainly driven by the fact that there was no chance to run multiple manufacturing batches to improve parameter results [9].

Similar decisions had to be made for the simulations. Therefore, all simulations for the parameter study were reduced to a 2D simulation with additional simplifications (e.g. on crack extension length). Fixing the crack growth increment to a static value made it impossible to calculate component lifetimes with the simulation.
In addition, the validation of the FE model by test points was only done with a small number of test references, as the simulation is very time-consuming and further investigations would have exceeded the time frame of the project. The simulation also did not permit estimation of spalling propagation or initiation; therefore, a starting point for crack propagation was required (initial crack based on maximum spalling depth).
As described in chapter 3.5 and above, there are limitations to be considered not only for the definition of specific parameter boundaries but also for the use of the developed simulation model in the future.
Nevertheless, this can be seen as a starting point for further research on these topics and an optimization and improvement of the results and tools gained from this research project.

Therefore, a list of recommendations for further research on this topic can be summarized as follows:

- Improve the simulation model to reduce calculation time and manual work for crack extension, including development of automations for the simulation process
- Analyze and study parameter limitations for real cases and applications based on the knowledge from this research project for a given and fixed manufacturing process (development of specific limitations for a given application) including material threshold value definition
- Improve manufacturing adjustments to meet additional/improved parameter levels (e.g. residual stress) or a wider range of parameter values
- Evaluate results for specific applications (e.g. planetary gears)
- Additional testing to obtain a better statistical background
- Evaluate a wider range of materials or additional treatments that could be beneficial for crack propagation
- Develop a standard for certification regulations to provide guidance to designers for all body-stress-critical applications

5. References

References for which the revision status is not provided refer to the last completely signed and therefore approved version.

[1] EASA, Procurement Document “Integrity improvement of rotorcraft main gear box (MGB)”, EASA.2019.HVP.17, 09/2019

[2] EASA/ZFL, Contract “Direct service contract for H2020 Project: Integrity improvement of rotorcraft main gear box (MGB), EASA.2019.C15, 16/06/2020

[3] D2-1: S. Hilleke, Technical Note “Review of the state-of-the-art design criteria for reliability and flaw tolerance in integrated bearing races and list of relevant design parameters identified”, 01 June 2021

[4] D2-2: S. Hilleke, Technical Note “Detailed analysis methodology”, 10 November 2021

[5] D2-3: W. Riesen “Stream 1: Summary and Conclusion report”, 06. October 2023

[6] D2-4: R. Boukellif, “Design parameters limitations for reliability and flaw tolerance”, 22. March 2023

[7] D2-5: R. Boukellif, “Critical threats and crack development”, 12. July 2023

[8] D2-6, W. Riesen, Test Instruction “Final Test Plan”, 26. May 2023

[9] D2-7: W. Riesen/R. Boukellif/S. Hilleke, “Test Report”, 21. February 2024

Bibliography

Project reports

- D1-1: W. Riesen, “Review of the state-of-the-art rotorcraft gearbox configuration and component designs”, 02 December 2021
- D1-2: W. Riesen, “Description and supporting evaluation of architecture and individual component design proposals, as well as determination of component/ sub-system design solutions”, 04. May 2023
- D1-3: W. Riesen “Stream 1: Summary and Conclusion report”, 06. October 2023
- D2-1: S. Hilleke, “Review of the state-of-the-art design criteria for reliability and flaw tolerance in integrated bearing races and list of relevant design parameters identified”, 01. June 2021
- D2-2: S. Hilleke, “Detailed analysis methodology”, 10. November 2021
- D2-3: W. Riesen “Stream 1: Summary and Conclusion report”, 06. October 2023
- D2-4: R. Boukellif, “Design parameters limitations for reliability and flaw tolerance”, 22. March 2023
- D2-5: R. Boukellif, “Critical threats and crack development”, 12. July 2023
- D2-6: W. Riesen, “Final Test Plan”, 26. May 2023
- D2-7: W. Riesen/R. Boukellif/S. Hilleke, “Test Report”, 21. February 2024

Annex A Key design parameter

Parameter	criticality	Rationale
Parameters suitable for all bearings		
Bearing type	low	The aim of this task is not to evaluate differences between bearing types
Tightening – Hoop Stress	low	Not present for integrated raceways
Roller raceway full contact & truncation	high	Stress peaks leading to higher risk of RCF
Contact Stress	high	High stress amplitudes leading to high risk of RCF. A main parameter contributing to the contact stress is the roller profile.
Misalignment	high	Misalignment leads to high local stress peaks and risk of RCF
Slippage and P.V.	high	Slippage leads to increased wear. In the event of crack initiation, it could lead to a load situation that initiates crack propagation
Lambda ratio lubrication	high	Ratio is directly linked to the risk of spalling and therefore to the reliability of the raceway
Oil flow	low	Oil flow is important for temperature management and only indirectly influences reliability
Oil cleanliness / pollution	high	Overrolling of particles is a main contributor to raceway damage and could lead to a reduction in the reliability of the raceway
Bearing life	low	Calculations are mainly based on ideal boundary conditions and are inaccurate in terms of reliability
Internal radial clearance and roller diameter	high	Direct influence on loading situation and contact stress (see also Contact stress)
Axial clearance and roller length	high	Direct influence on loading situation and contact stress (see also Contact stress).
Cage pocket clearance	high	Direct influence on loading situation and contact stress (see also Contact stress)
Oscillation	high	Impact on full contact / edge contact (see also Roller raceway full contact & truncation)
Inner or outer ring diameter	low	Negligible for integrated raceways
Contact angle	medium	Direct influence on sliding rate and contact pressure with potential risk of RCF. As it is only relevant while exceeding the design contact angle, it is ranked as “medium”.
Roller geometrical tolerance	medium	Influences lubrication efficiency; minor influence in comparison to other geometrical parameters and therefore medium
Roller diameter roughness	medium	Direct influence on lubrication efficiency (see also lambda lubrication ratio)
Roller face roughness	medium	Direct influence on sliding of the rolling element and consequently the loading situation. Usually the economically possible limits of

Parameter	criticality	Rationale
		manufacturing are already reached, so no great impact of additional optimization is expected. Therefore it is ranked as medium.
Cage pocket geometry	medium	Influences loading situation but smaller than axial clearance
Cage guide diameter and cage landing clearance	low	No direct influence on the raceway, but does influence the reliability of the cage
Rings/shaft/gear raceway roundness and location	low	Complementary to roller geometrical tolerances
Rings/shaft/gear raceway profile	medium	Complementary to roller profile
Rings/shaft/gear raceway roughness	medium	Complementary to roller diameter roughness
Roughness of cage piloting surface on ring/shaft/gear	low	Complementary to guide diameter and cage landing clearance
Material and material cleanliness and composition	high	Material has a major effect on fatigue limit and fracture toughness but is generally not freely selectable. It is not within the scope of this project to fully characterize the impact of all different characteristics that may be impacted by the material selected with regards to bearing reliability and flaw tolerance. The material cleanliness (melt quality) defines the number of potential crack initiation locations. The material composition has an influence on the microstructure and potential crack initiation locations.
Hardness	high	Hardness has direct influence on the mechanical properties of the steel and can contribute to cracks or spalling.
Case hardening depth	high	Mechanical properties of the steel change at the end of the hardening zone and can influence the flaw tolerance.
Residual Stress	high	Change in stress level could lead to decreased flaw tolerance
Parameters particular to bearings with integrated raceways		
Body stress	high	Generally higher stress level due to superposition of loads at the raceway compared to conventional bearings with non-integrated raceways. The higher stress level increases the risk of spalling and crack initiation.
Material and surface treatment	high	The selection of the material and the corresponding heat treatment process influences the stress state and the resistance to damage and flaws.
Parameters for planetary gears with integrated raceways		
Rim thickness	high	As demonstrated in previous research studies, rim thickness directly influences the loading and stress situation of the gear. A thin rim leads to an ovalization of the gear with a higher stress level and a combination of bending, shear and normal load.

Parameter	criticality	Rationale
Contact ratio and tooth root stress (linked to body stress)	high	The body stress for planetary gears has a high criticality, as it does for integrated gears in general. The contact ratio influences the stress state and level in the gear and directly affects the body stress. For thin-rimmed planetary gears, the body stress is mainly driven by the ovalization, and high contact ratios can even lead to a stress increase (reduced rim thickness due to increased dedendum height). The tooth root stress may also affect the general body stress in combination with thin rimmed planetary gears.
Width of load zone (load sector) and number of rolling elements	high	The width of the load zone (load sector) and the number of rolling elements have a direct influence on stress state and level and also on the level of ovalization of the gear. A similar effect was described for the parameter rim thickness and the axial clearance. Ovalization is mandatory for reliability and flaw tolerance.

Table 2: Summary and classification of selected design parameters (criticality for reliability and flaw tolerance of bearing races)

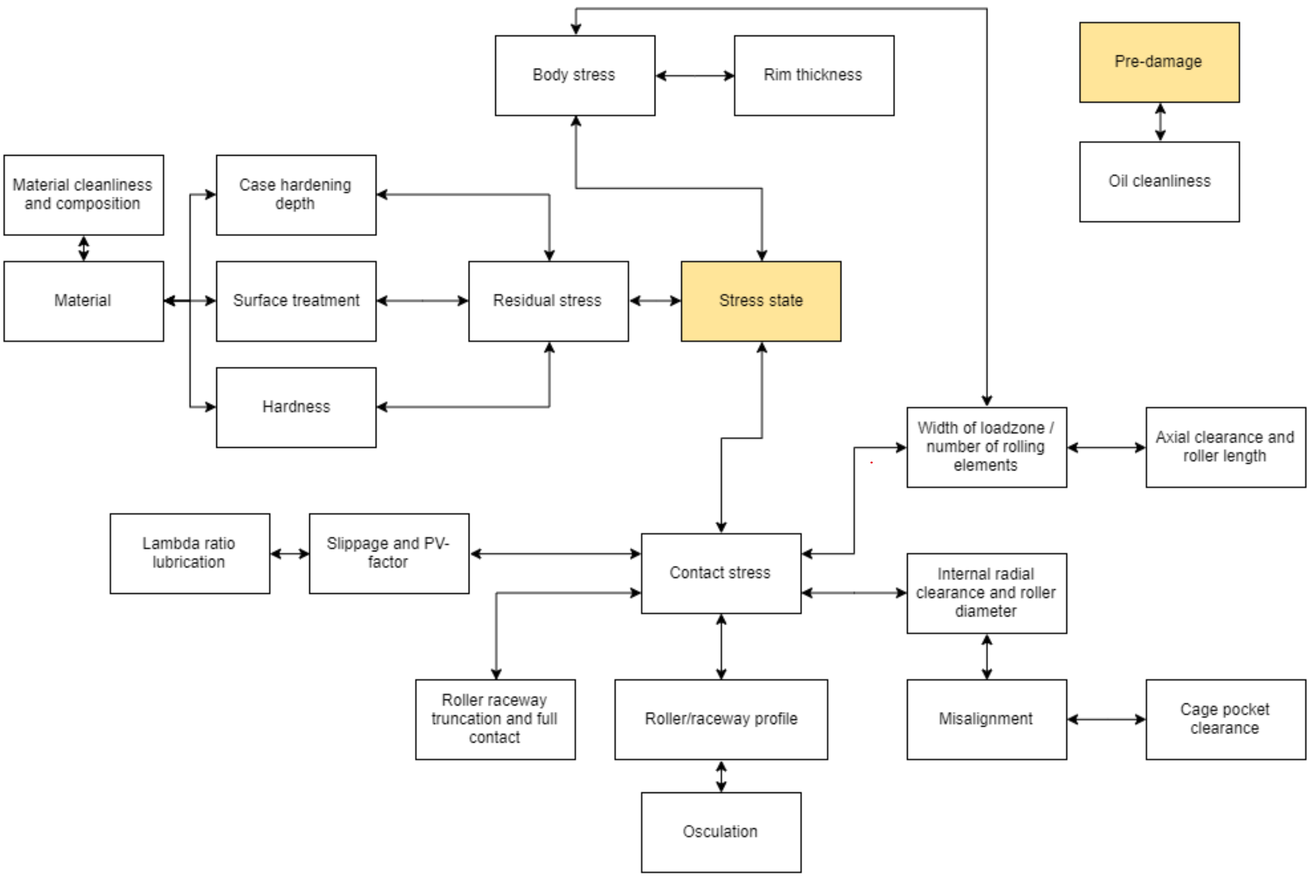

Figure 5: Interaction of critical parameters

Annex B Prioritization of parameter

Priorization of design parameter for testing according to crack initiation phase I

	Parameter categories			
Test capacity & experience	**Contact stress**	**Contact stress / Body stress**	**Body stress**	**Residual stress**
1 (high)	Contact pressure			Material
	Lambda ratio lubrication			
2	Roller raceway truncation and full contact	Axial clearance and roller length	Rim thickness	Surface treatment
	Roller / raceway profile			Case hardening depth
	Osculation	Width of loaded zone (load sector) and number of rolling elements		
	Internal radial clearance and roller diameter			
	Contact angle			
3	Misalignment			Hardness
	Raceway / roller roughness			Residual stress
4 (low)	Slippage and P.V.-factor		Contact ratio and tooth root stress	
	Cage pocket clearance		Body stress (e.g. complex load)	
	Oil cleanliness			

	chosen key design parameter
xxx	fixed
xxx	variable

Table 3: Prioritization of parameters to be analyzed for crack initiation

Priorization of design parameter for testing according to crack propagation phase II

	Parameter categories			
Test capacity & experience	**Contact stress**	**Contact stress / Body stress**	**Body stress**	**Residual stress**
1 (high)	Contact pressure			Material
	Lambda ratio lubrication			
2	Roller raceway truncation and full contact	Axial clearance and roller length	Rim thickness	Surface treatment
	Roller / raceway profile			Case hardening depth
	Osculation	Width of loaded zone (load sector) and number of rolling elements		
	Internal radial clearance and roller diameter			
	Contact angle			
3	Misalignment			Hardness
	Raceway / roller roughness			Residual stress
4 (low)	Slippage and P.V.-factor		Contact ratio and tooth root stress	
	Cage pocket clearance		Body stress (e.g. complex load)	
	Oil cleanliness			

	chosen key design parameter
xxx	fixed
xxx	variable

Table 4: Prioritization of parameters to be analyzed for crack propagation

Annex C Simulation model: Design limitation development

C.1 FE model description

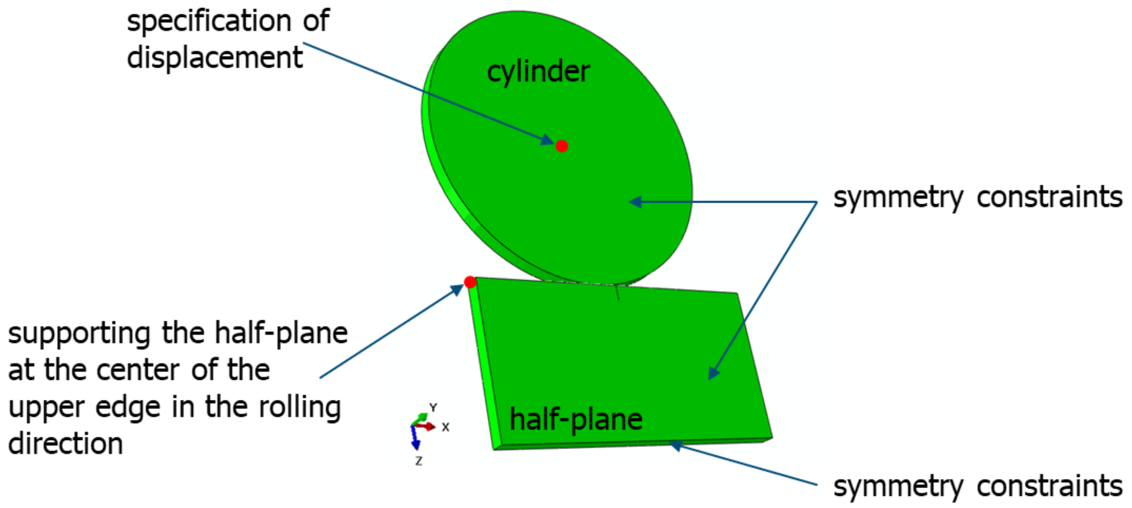

Figure 6: Kinematic boundary conditions at cylinder and half-plane

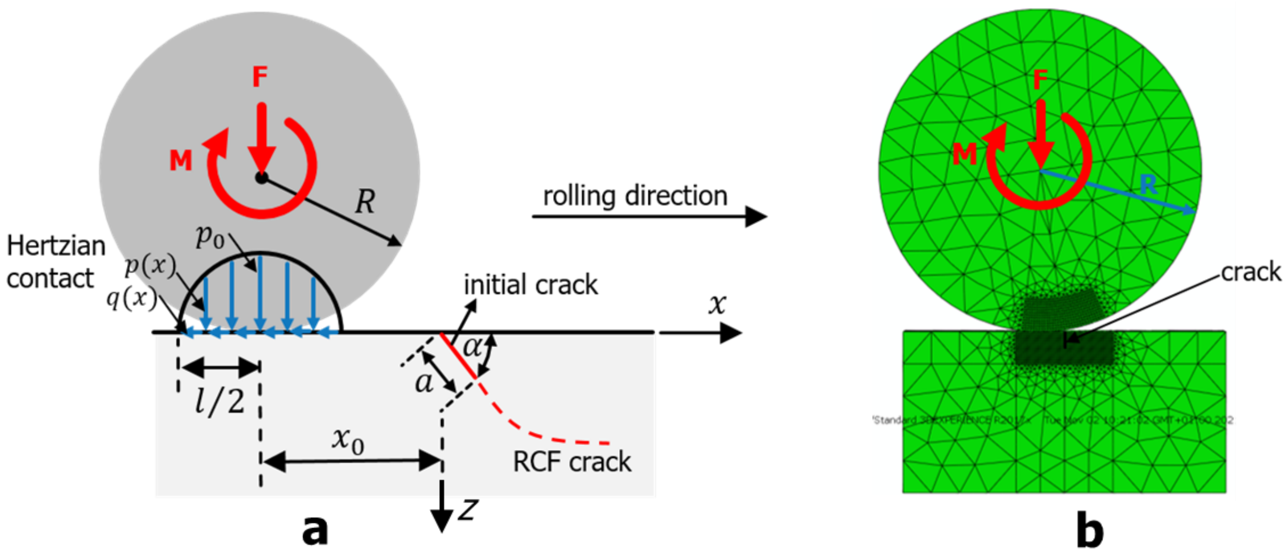

*Figure 7: Definition of crack parameters and FE geometry with mesh refinements: **a)** theoretical model, **b)** FE model for simulating rolling contact on a half-plane with crack length a = 1 mm and crack inclination $\alpha = 90°$*

C.2 FE model validation

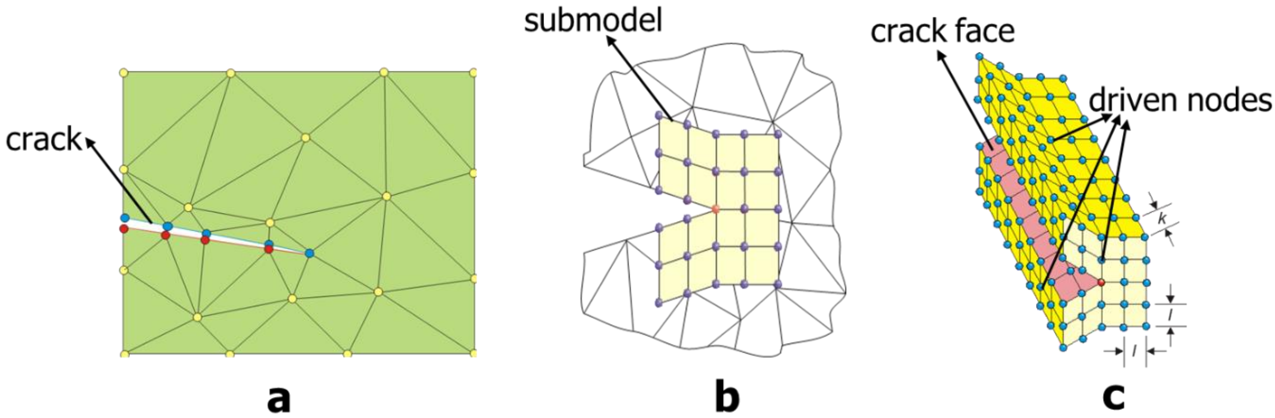

*Figure 8: Creating a submodel for FE fracture-mechanical evaluation: **a**) crack in global model, **b)** definition of the submodel, **c)** submodel with driven nodes*

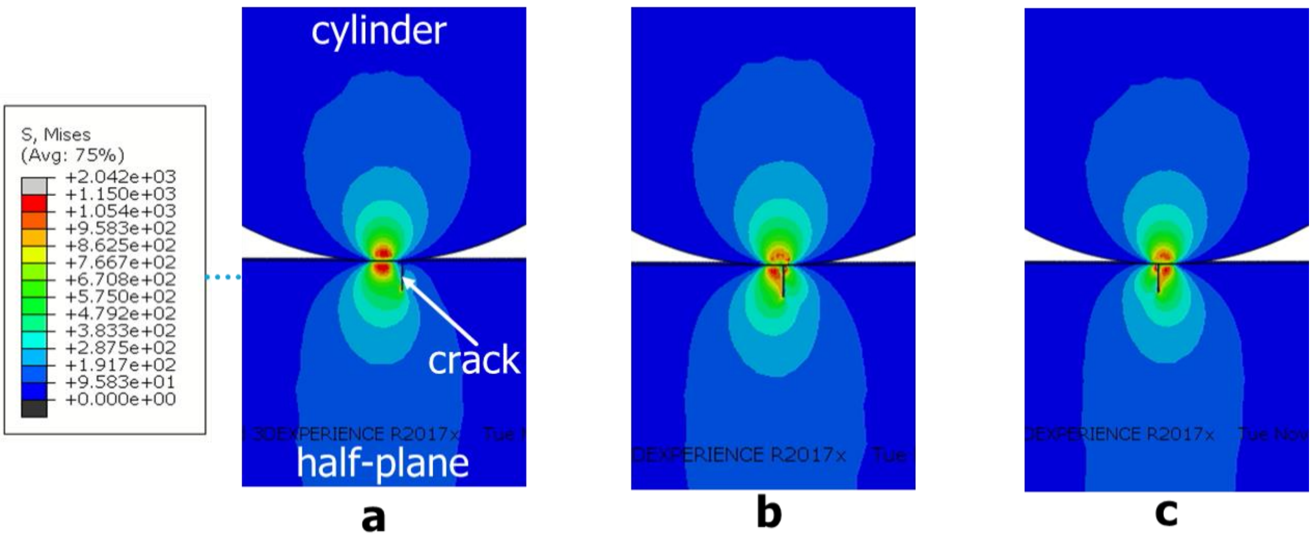

*Figure 9: Snapshot of stress field σ_{Mises} during the rollover process: **a)** before crack; **b)** close to the crack (before); **c)** close to the crack (after), and influence of Hertzian pressure on crack for the first example*

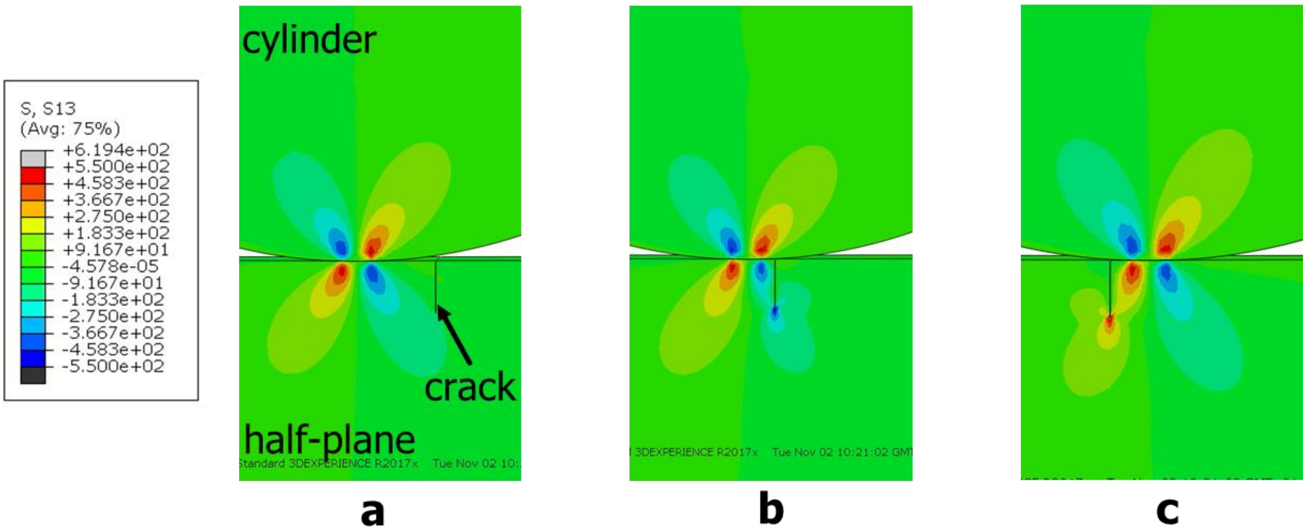

*Figure 10: Snapshot of shear stress field σ_{13} during the rollover process: **a)** before crack; **b)** on crack; **c)** after crack, alternating shear stress at the crack before and after crack rollover*

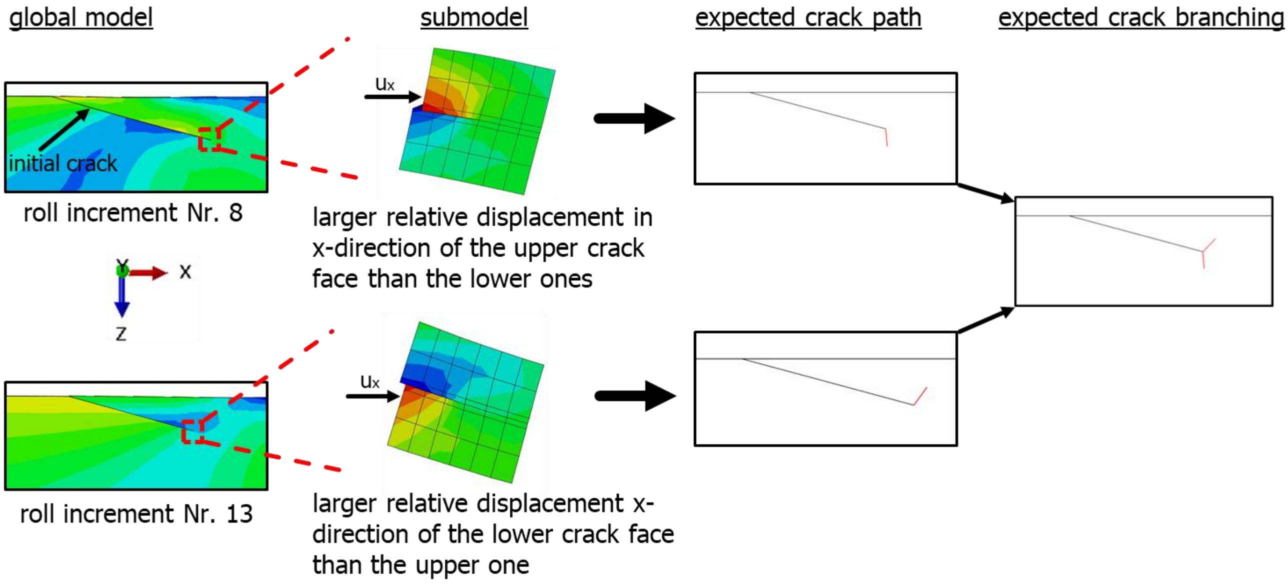

Figure 11: Description of the displacement at crack faces and crack branching at the crack tip

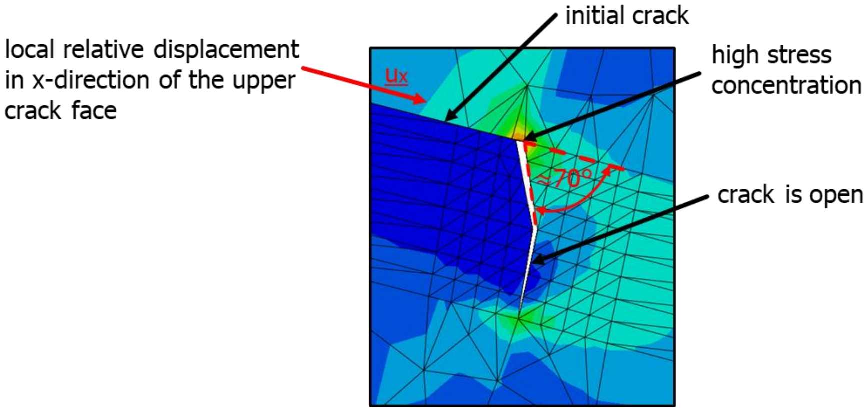

Figure 12: Description of the Mode I loading that occurs due to crack opening

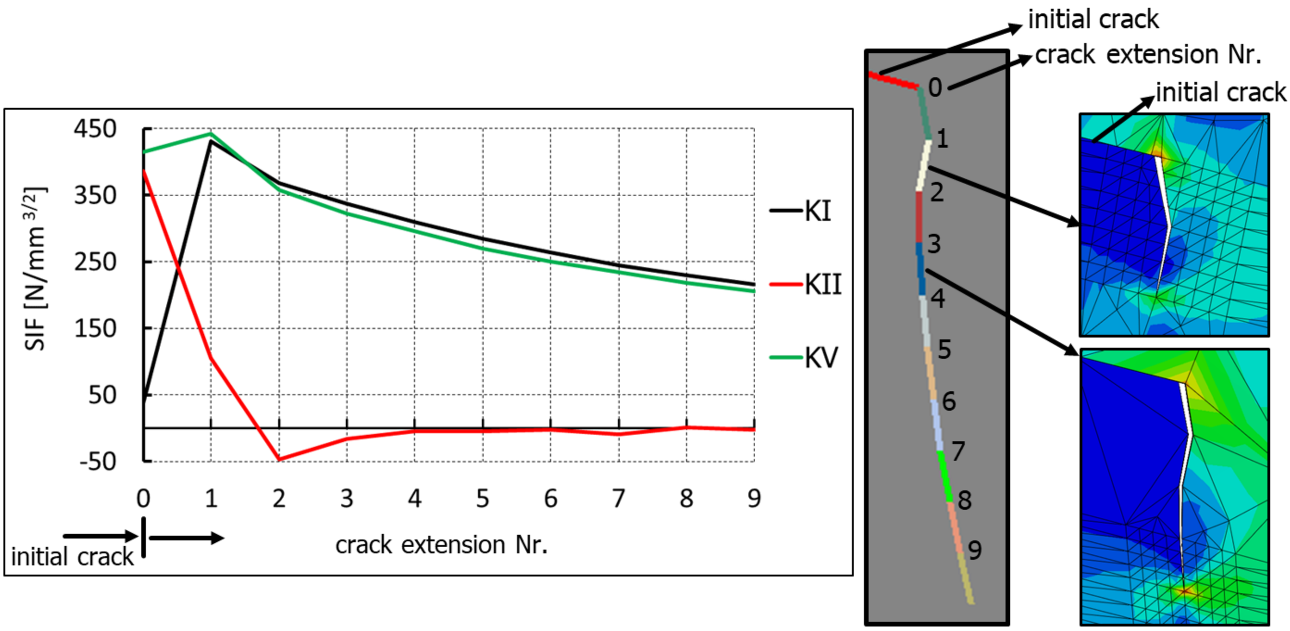

Figure 13: Curve of the SIFs K_I, K_{II} and K_V at roll increment 8 and the associated crack paths due to rolling contact in case of an inclined initial crack (crack length 1 mm, crack inclination 15°)

C.3 Parametric study

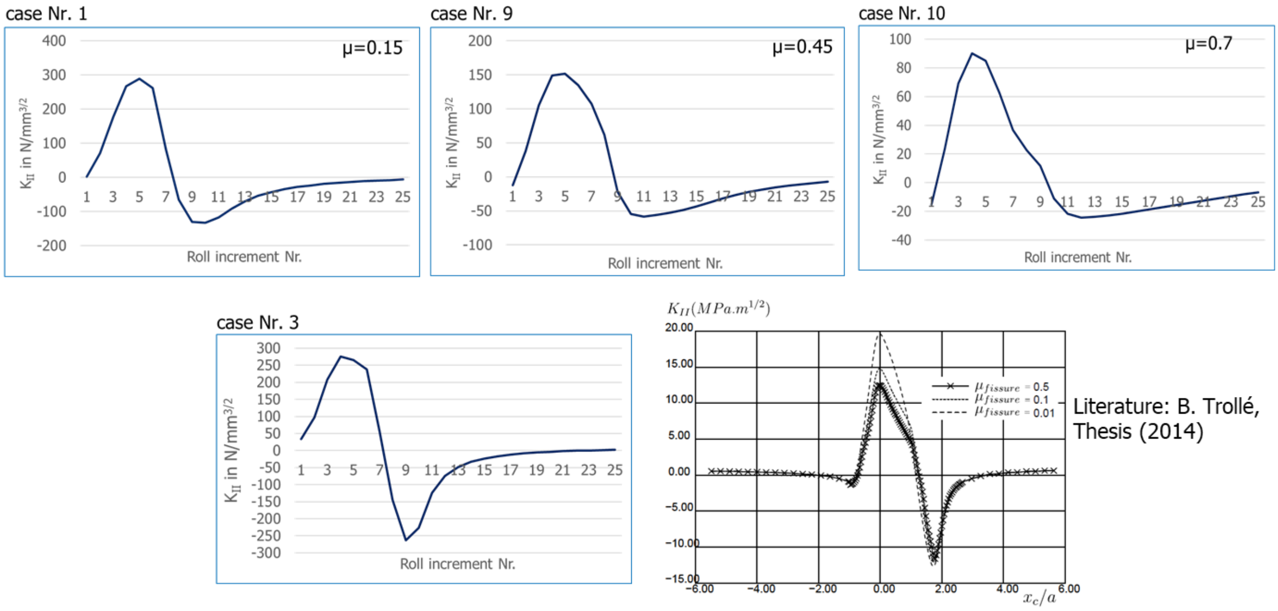

Figure 14: Comparison of the results with literature, effect of the friction coefficient of crack faces μ on the calculated curve of K_{II} in cases 1, 9 and 10: the initial crack angle is different from the simulation and the literature (top); curve of K_{II}: the initial crack angle from the simulation and literature is the same (below)

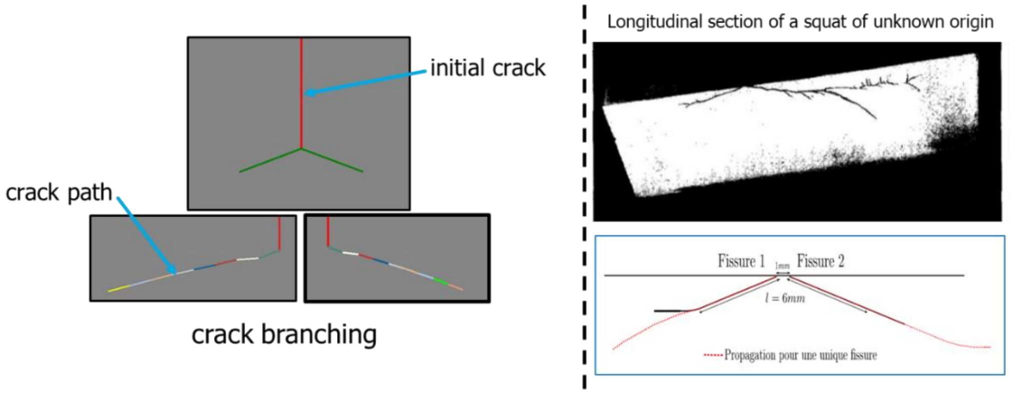

Figure 15: Comparison of the FE-results of the crack branching from case 4 (left) and the literature (right)

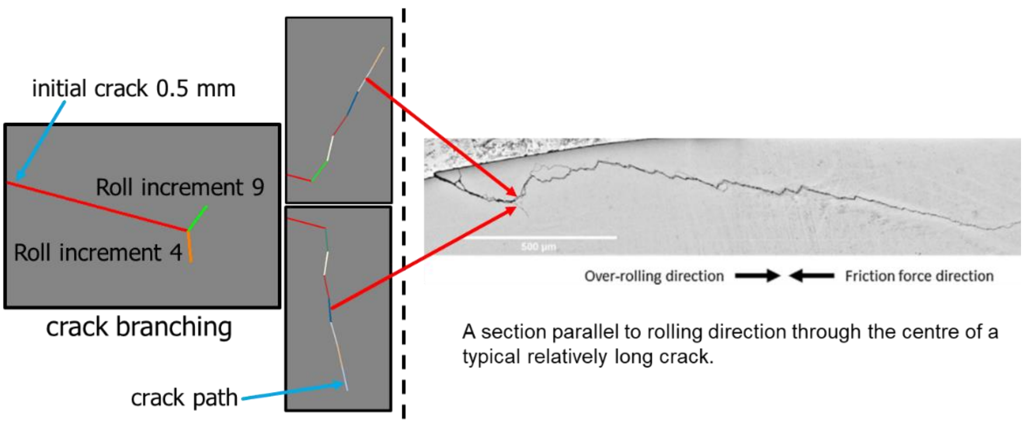

Figure 16: Comparison of the crack branching FE results between case 3 (left) and the literature (right)

Annex D Simulation model: Critical threats and crack development

D.1 FE model description

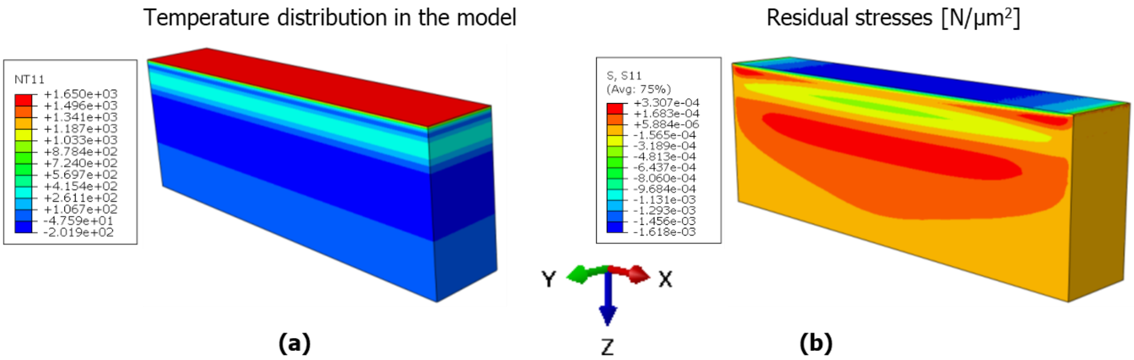

Figure 17: Modeling of residual stresses due to thermal stresses, (a) temperature distribution in the model, (b) residual stresses

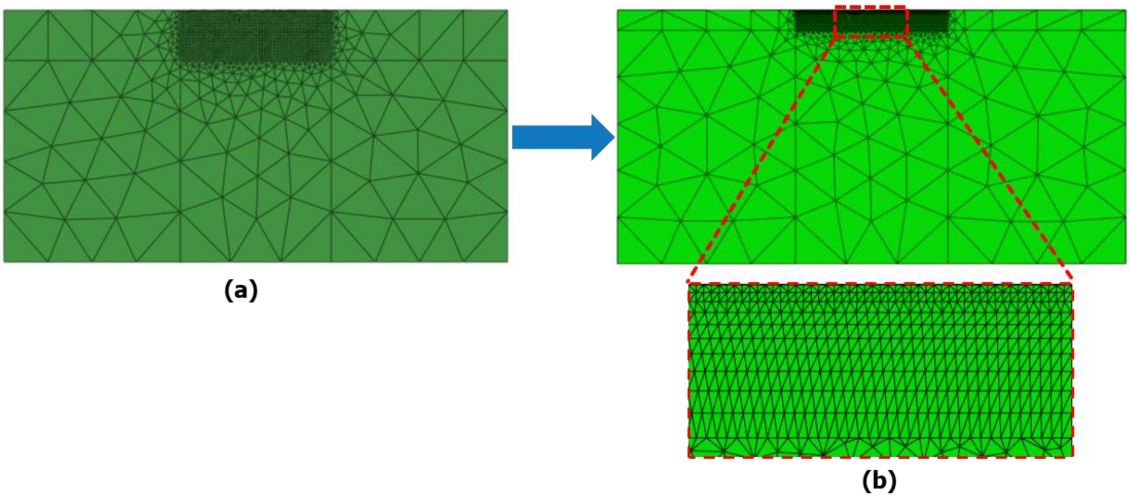

Figure 18: Description of the mesh used: (a) meshing of the half-plane used in D2-4, (b) new meshing of the half-plane to depict the high residual stress gradients in Z-direction

D.2 FE model validation

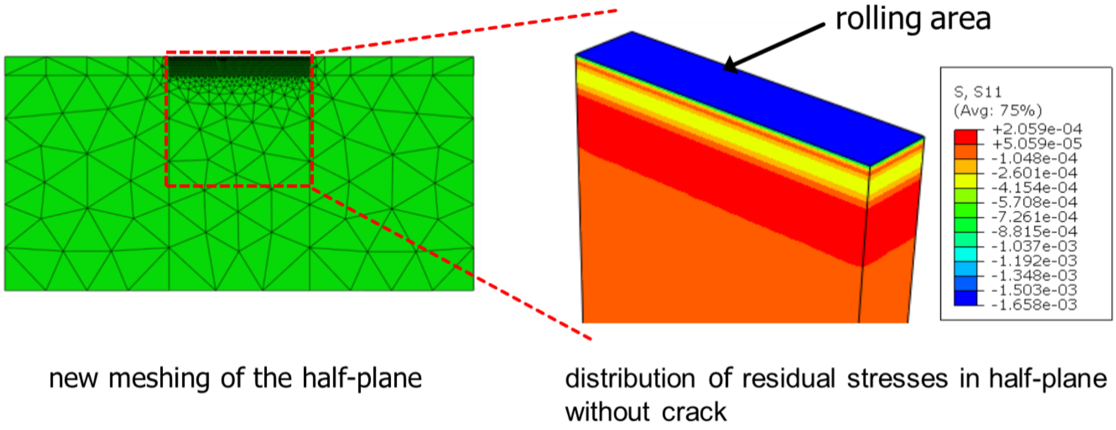

Figure 19: Implementation of the specified residual stresses by using the new mesh

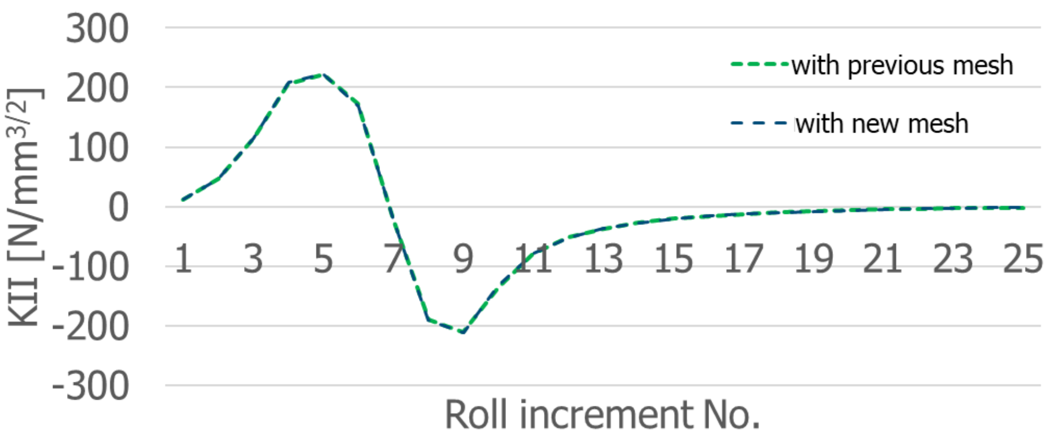

Figure 20: Comparison of the calculated stress intensity factors K_{II} with the new and previous mesh from D2-4

D.3 Parametric study

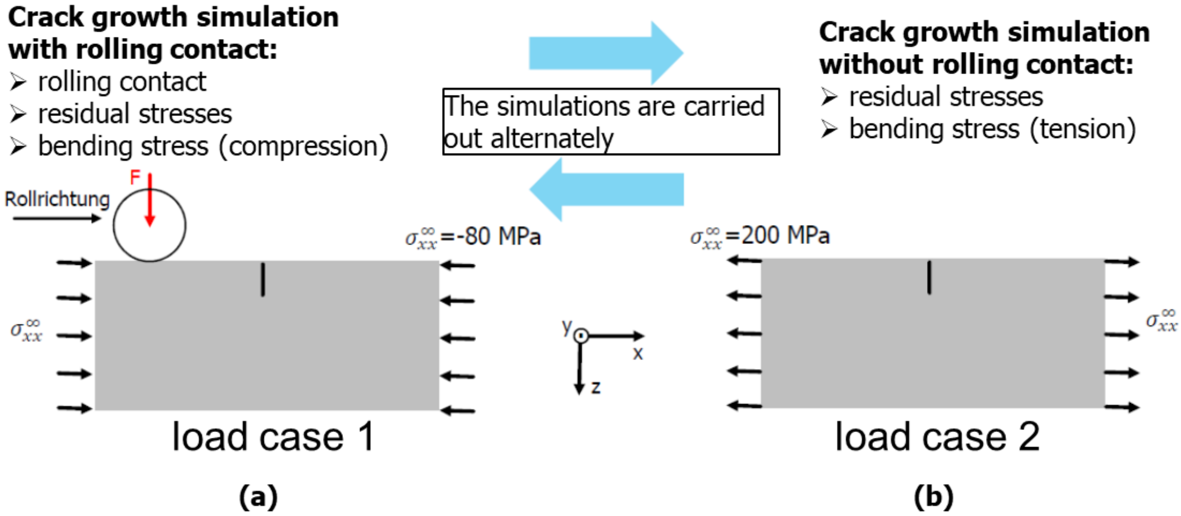

Figure 21: Crack growth simulation under additional bending stresses

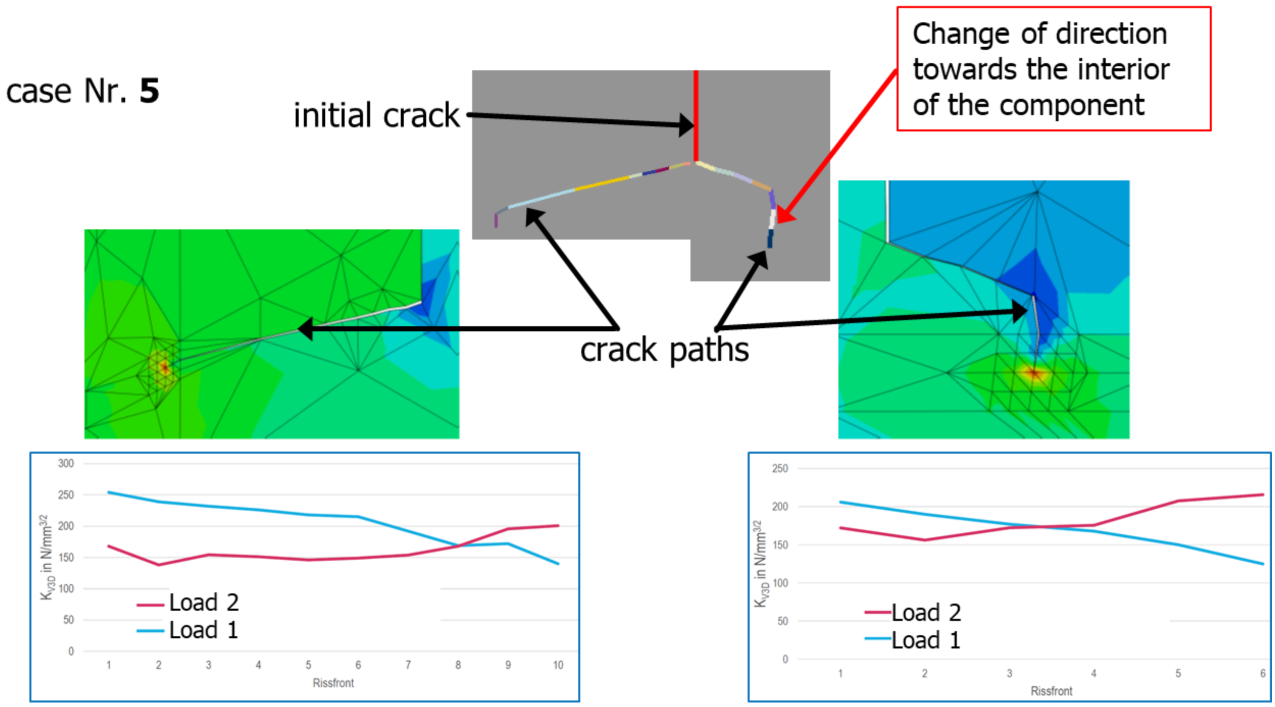

Figure 22: Comparison of the results due to load 1 and load 2, crack branching, left and right crack paths and K_V due to the rolling process and residual stresses, and complex load

D.4 Complex load

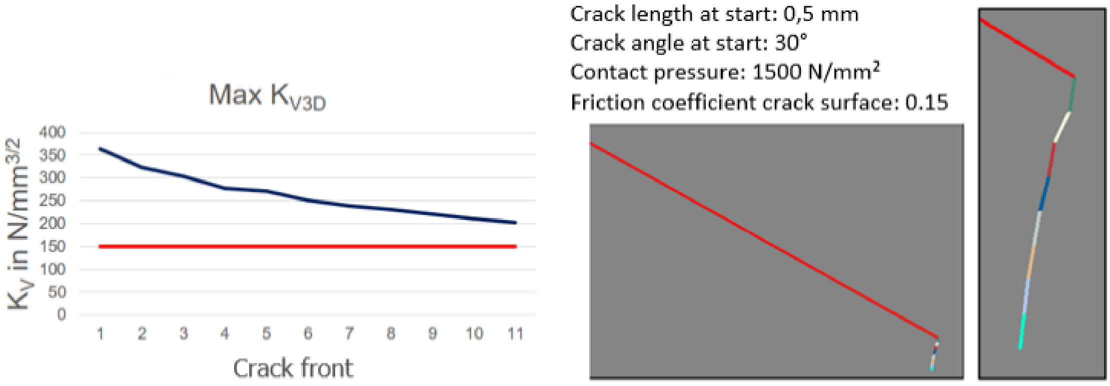

Figure 23: Example of crack simulation for a contact pressure of 1500 N/mm2

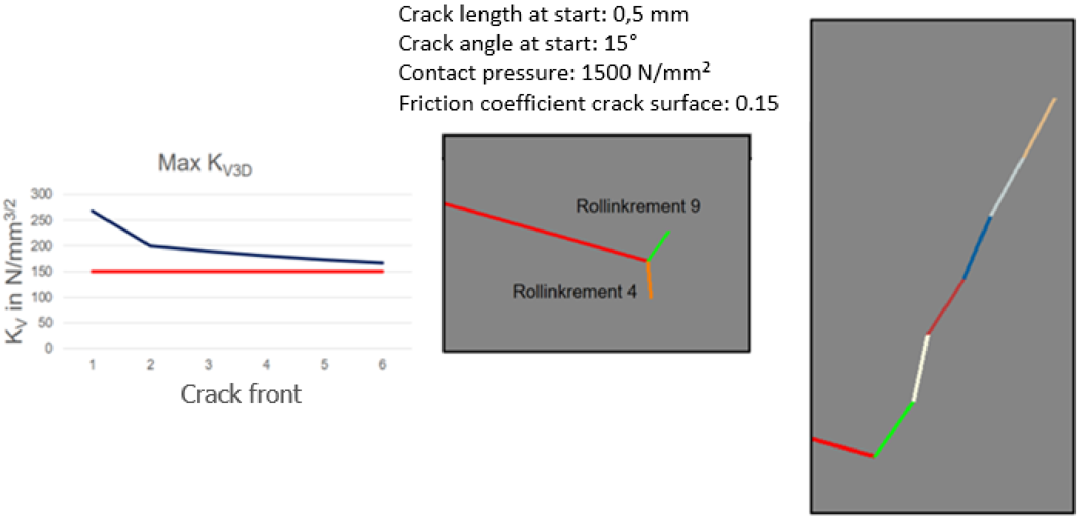

Figure 24: Example 1 of simulations for crack kinking at 1500 N/mm2 contact pressure

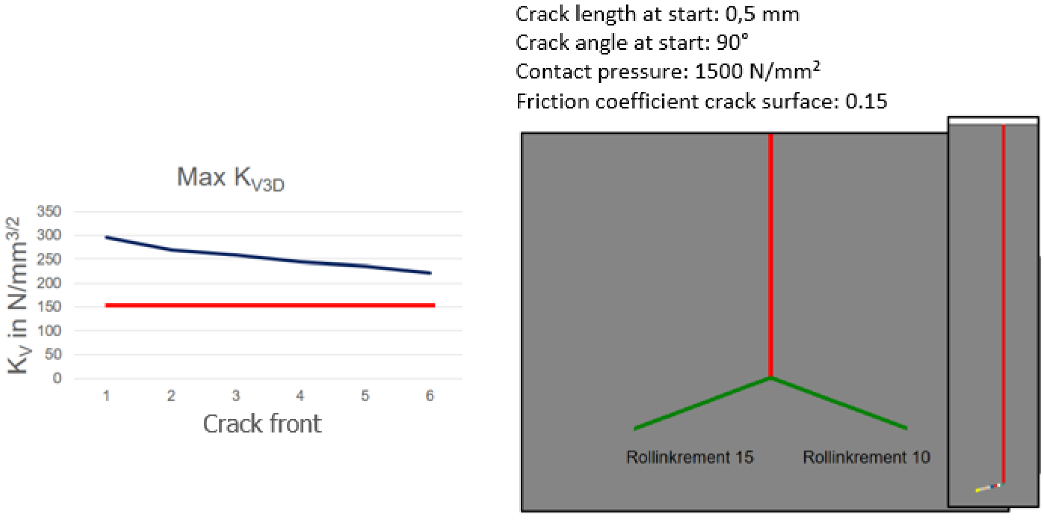

Figure 25: Example 2 of simulations for crack kinking at 1500 N/mm2 contact pressure

D.5 Validation of test results

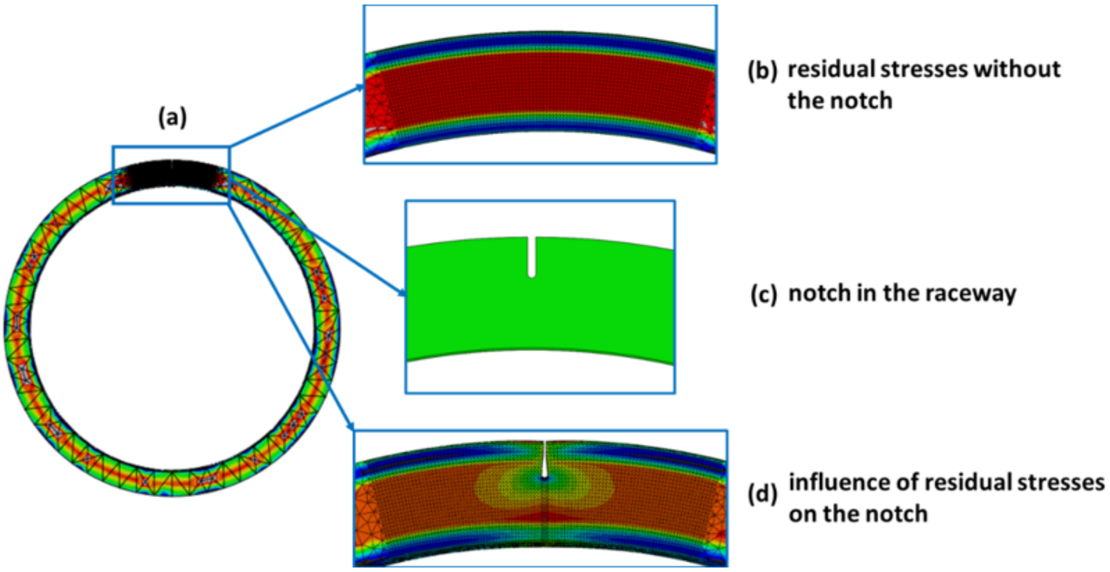

Figure 26: Implementation of residual stresses and notch as crack initiation for the shaft application

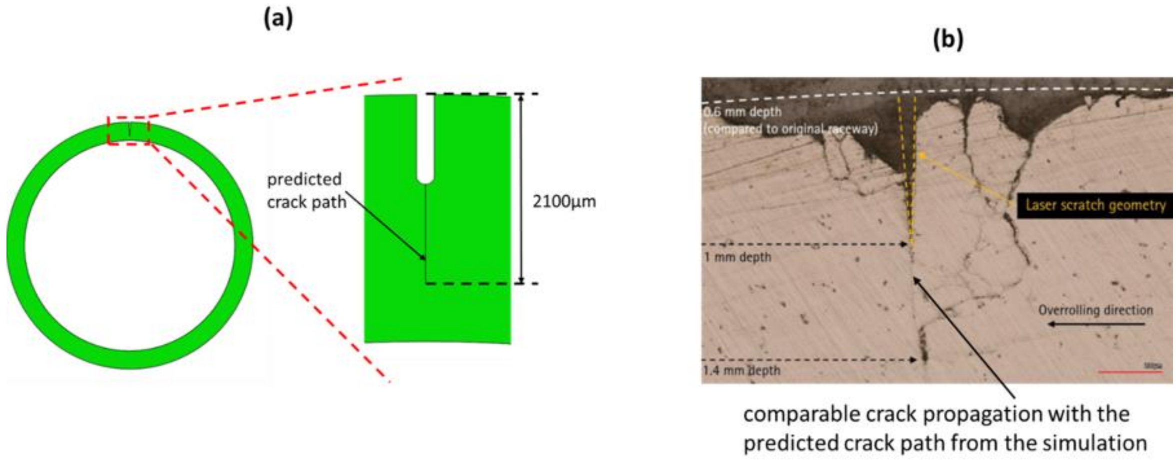

Figure 27: Comparison of predicted crack with results of testing for the shaft application

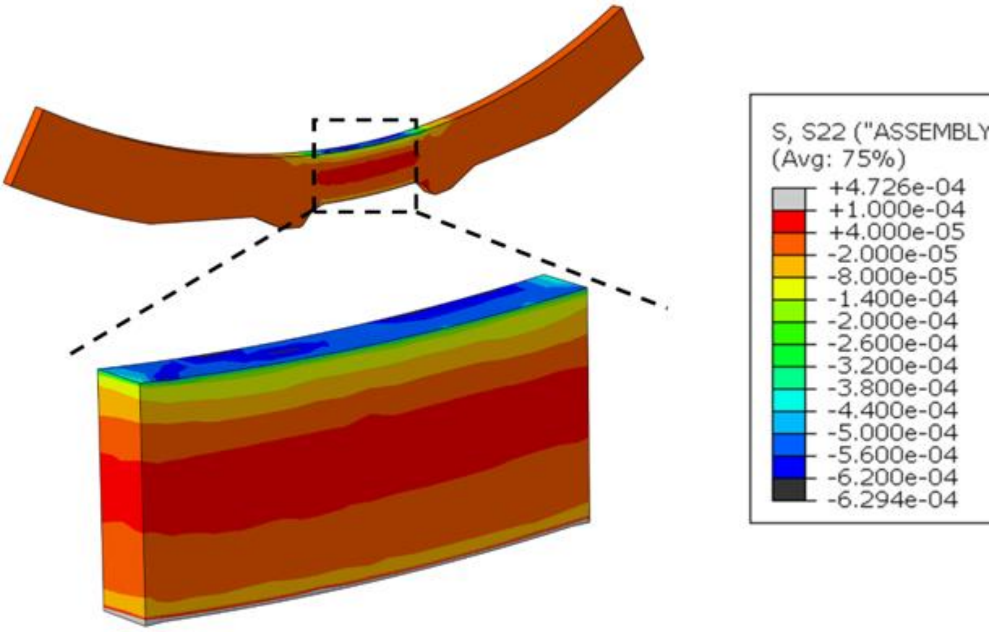

Figure 28: Implementation of residual stress profile for the outer ring application

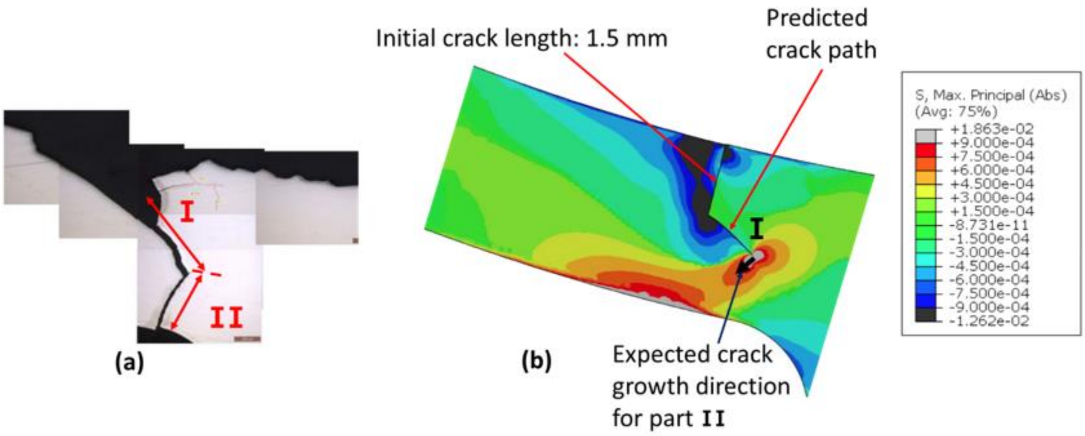

Figure 29: Comparison of predicted crack with results of testing for the outer ring application

Annex E Specimens and test benches

E.1 Outer Ring – Test campaign

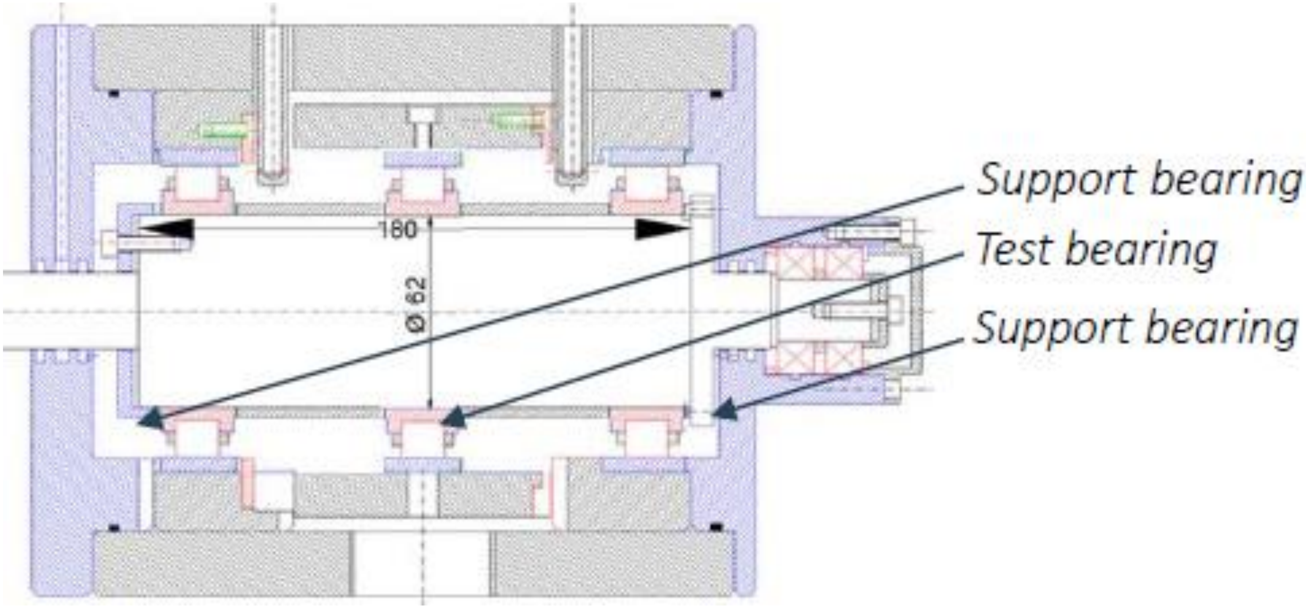

Figure 30: Test bench '1' test head

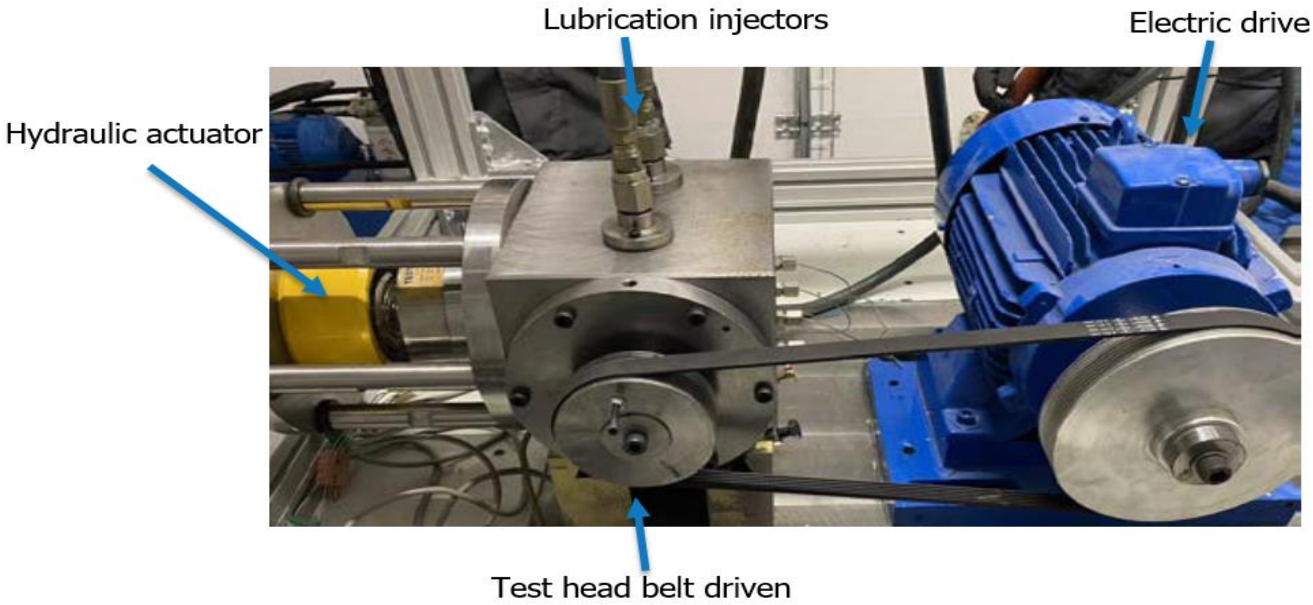

Figure 31: Test bench '1'

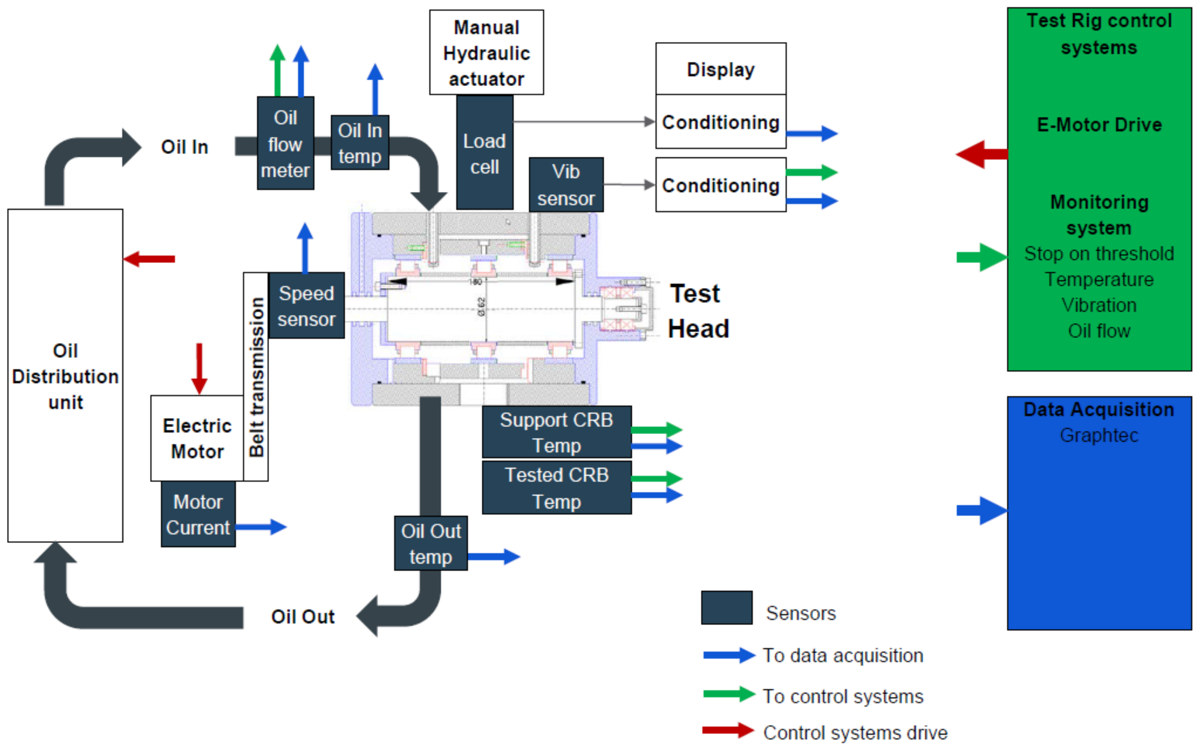

Figure 32: Test bench '1' monitoring and control system (schematic view)

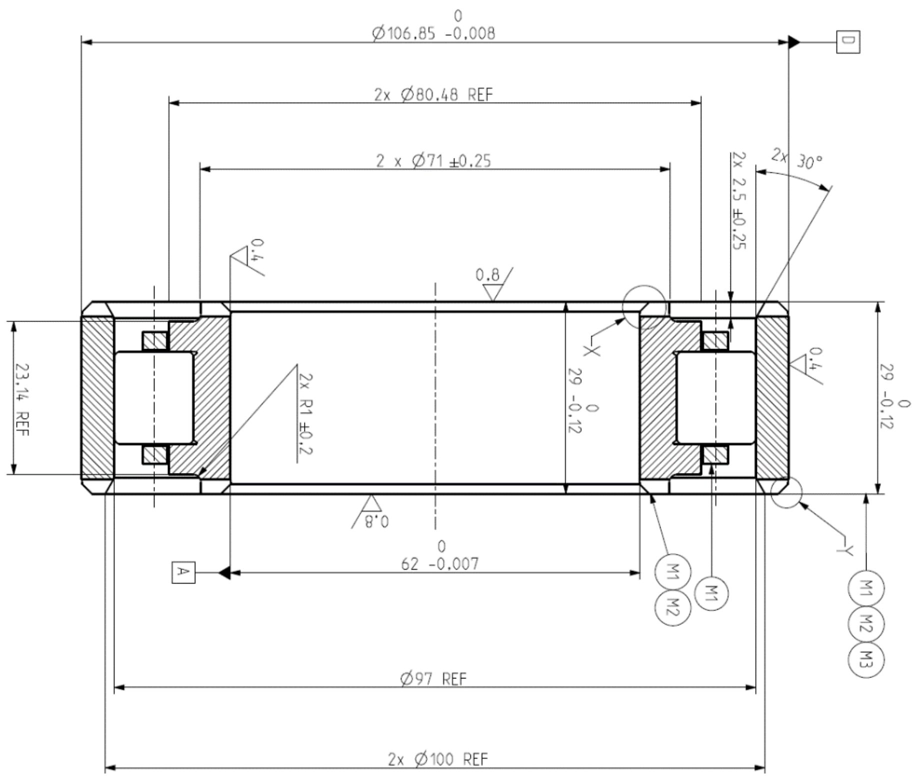

Figure 33: OR test specimen dimensions for test bench '1'

Figure 34: Picture of raceway with scratch before start of testing

Width	Depth	Shoulder height
175 -/+18 µm	20 -/+2 µm	3 to 12 µm

Table 5: Scratch dimensions for outer ring

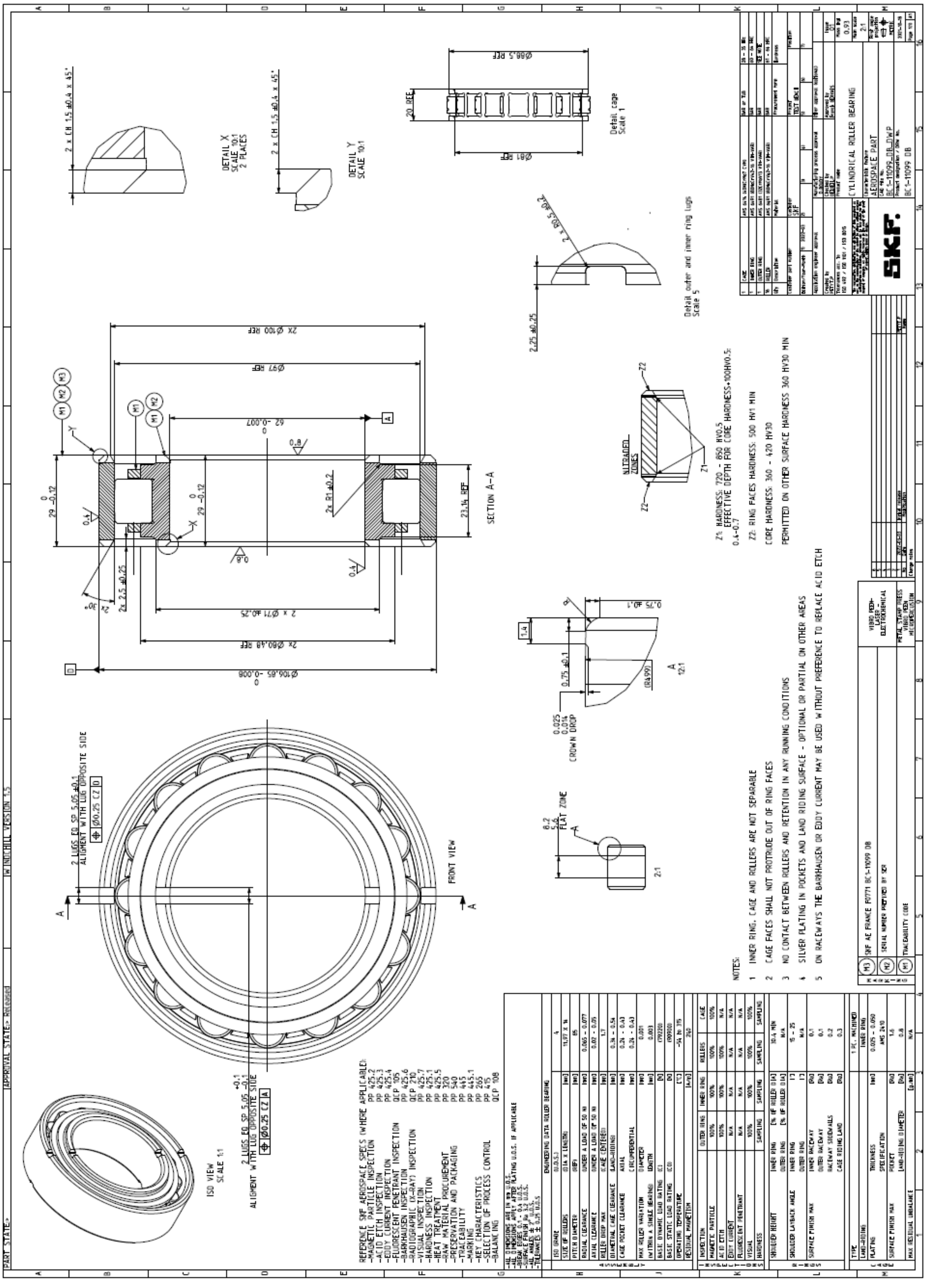

Figure 35: Detailed view of specimen for test bench ‘1’

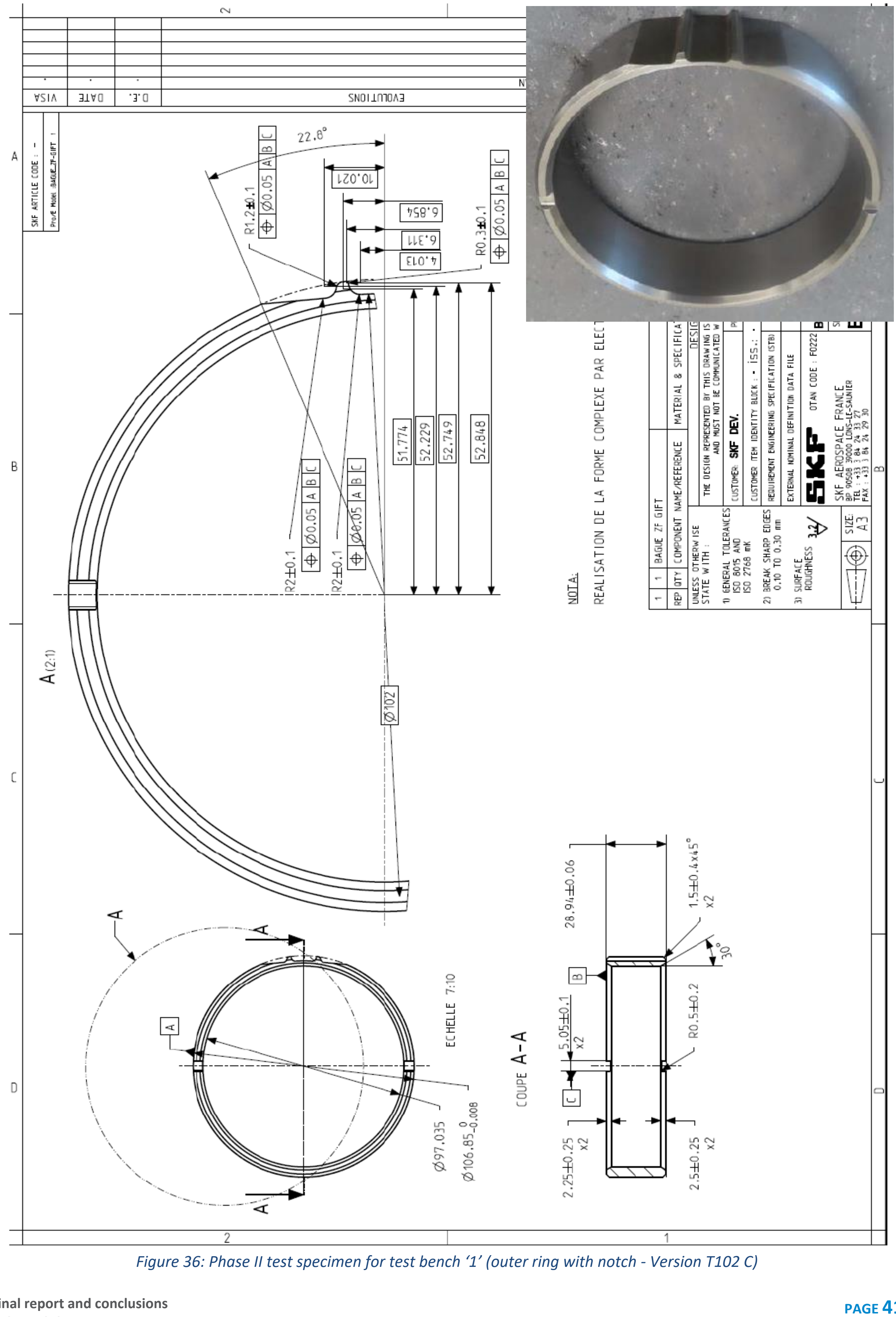

Figure 36: Phase II test specimen for test bench '1' (outer ring with notch - Version T102 C)

E.2 Shaft

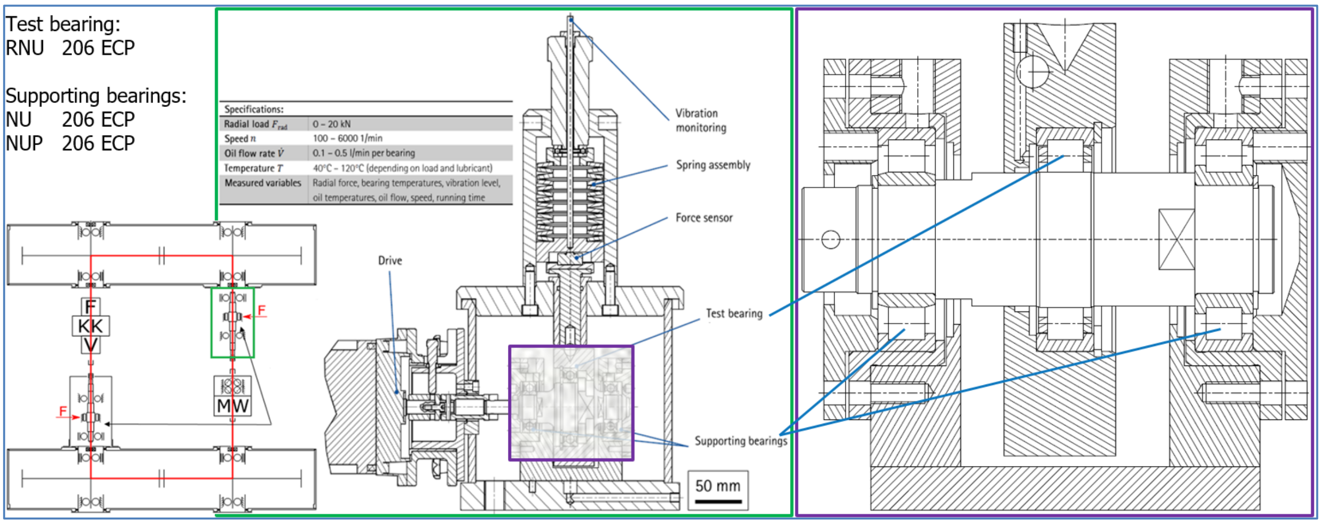

Figure 37: Test bench and test head '2' (schematic view)

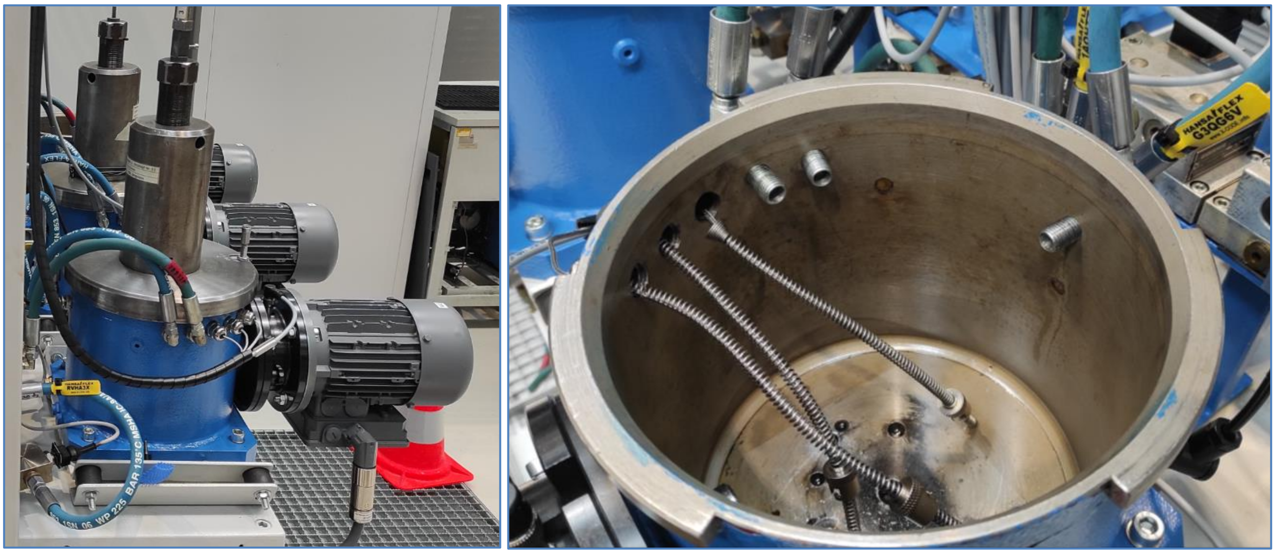

Figure 38: Test bench and test head '2'

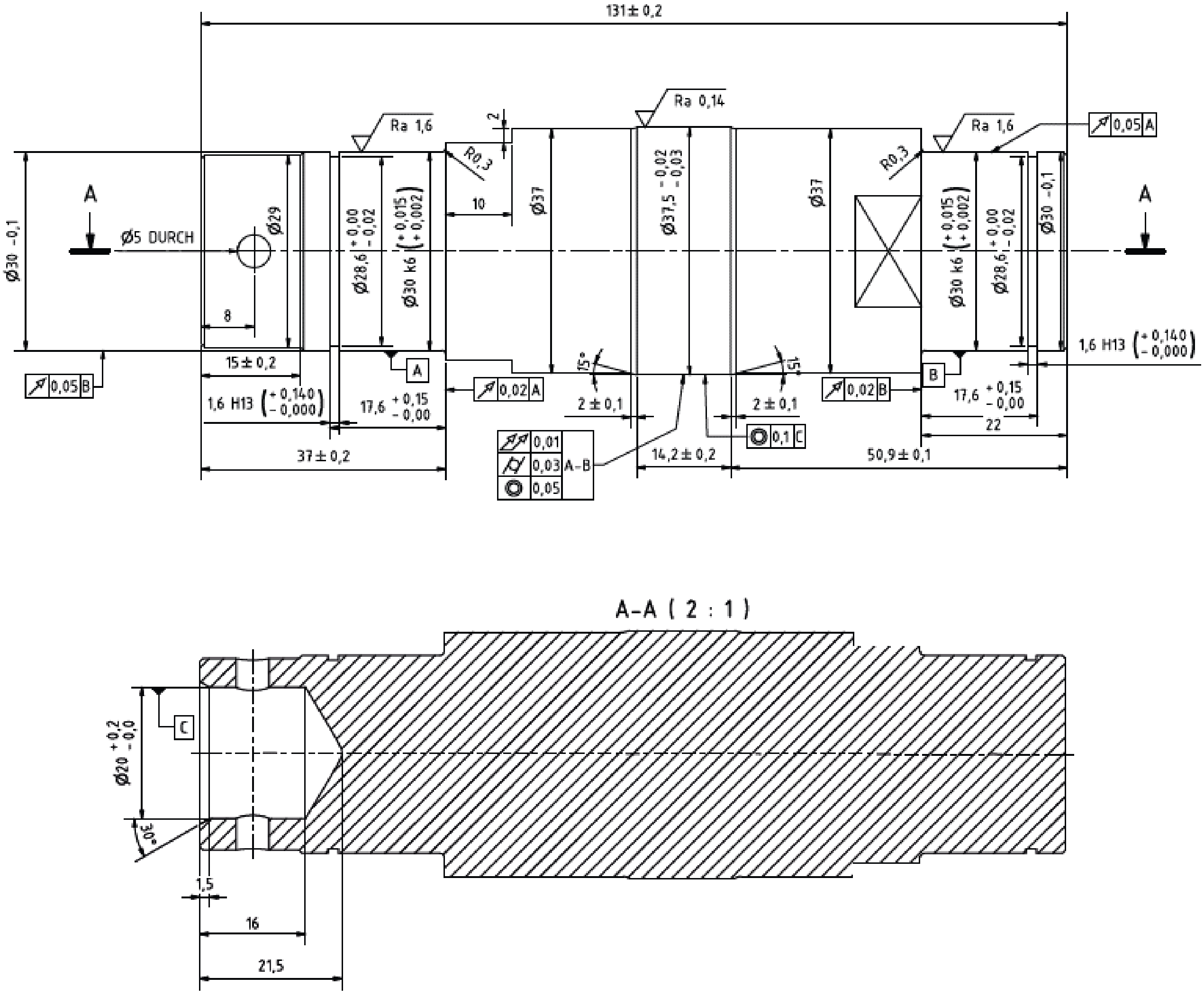

Figure 39: Phase I test specimen for test bench '2' (solid shaft)

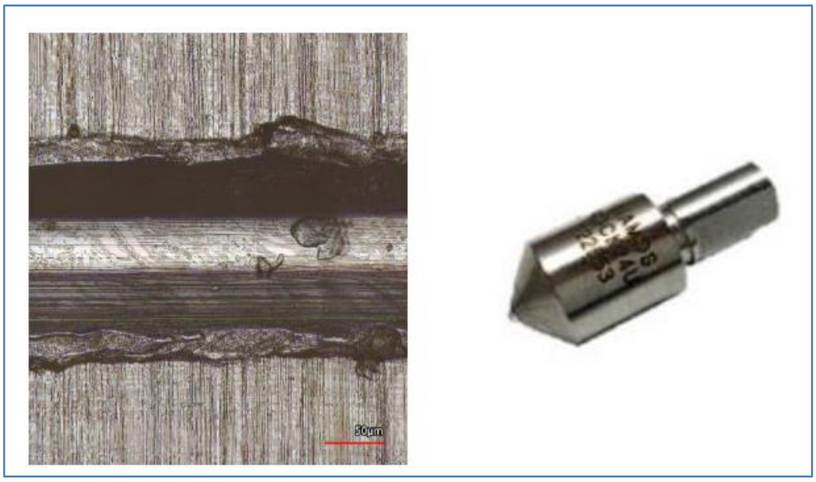

Figure 40: Indenter with scratch on raceway

Depth	Shoulder high	Width without shoulders	Width with shoulders
23.8 µm	18.7 µm	83.6 µm	200.5 µm

Table 6: Dimensions of scratch for shaft specimens

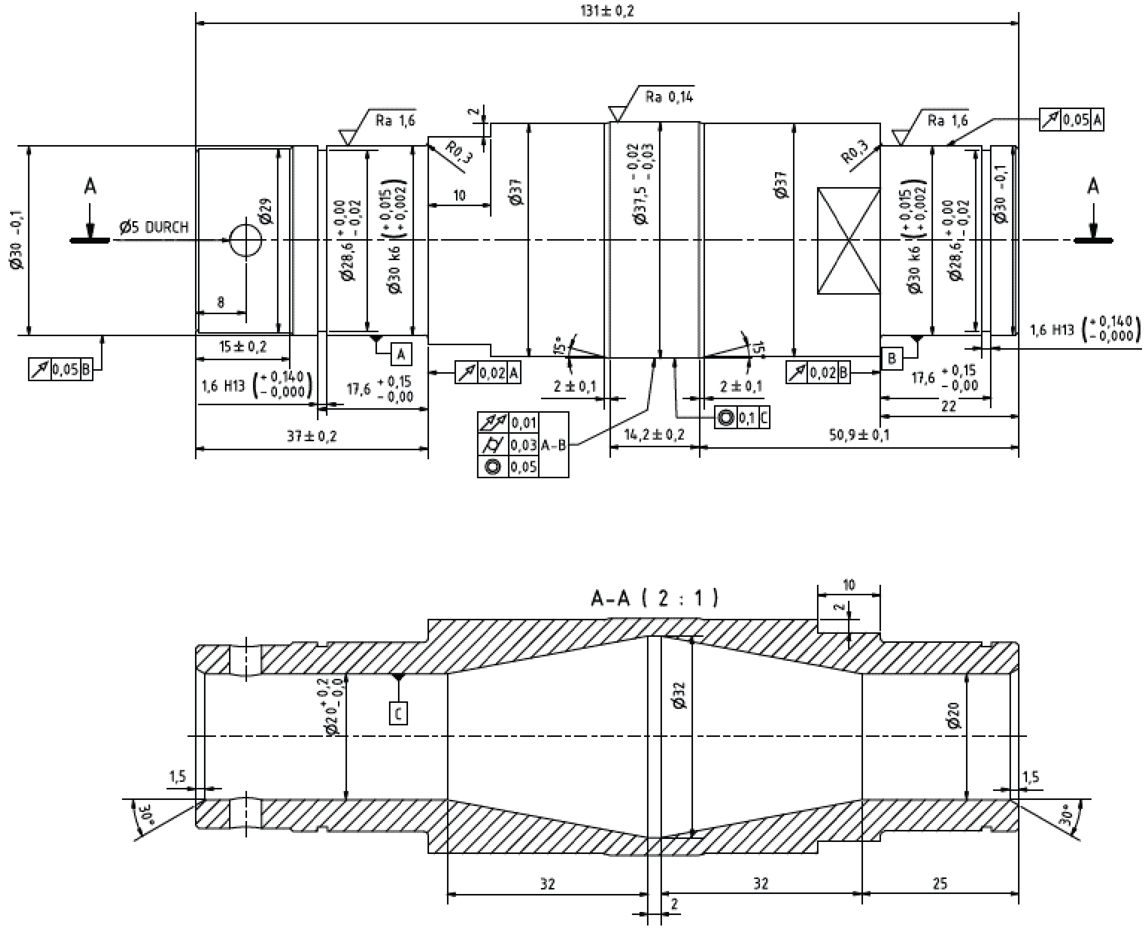

Figure 41: Phase II test specimen for test bench '2' (hollow shaft)

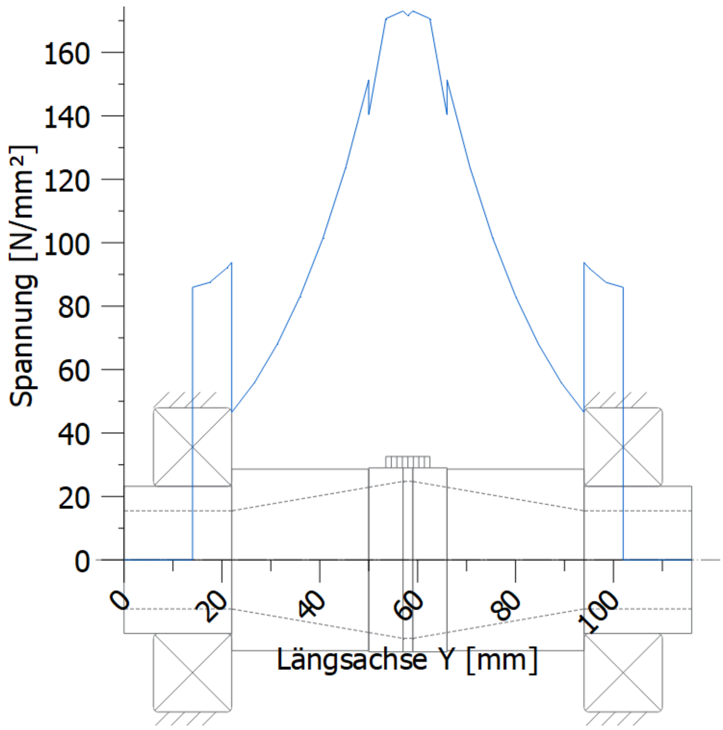

Figure 42: Bending stress profile for hollow shaft

Annex F - Summary of test results

Test phase	Material	Specimen	Version	Treatment/ Surface variant	Quantity	Contact Pressure	Cycles reached	Damage (visual inspection)
Phase I.1	M50Nil	Ring	B-Version 1	Baseline	3	2400 MPa	115.1 M. 179.2 M. 55.5 M.	Surface: spalling
	M50Nil	Ring	B-Version 1		1	1800 MPa	200 M.	n/a
	M50Nil	Ring	B-Version 1		0	1500 MPa	Canceled	n/a
	16NCD13	Shaft	V1 V1 V1		3	2400 MPa	127.5 M. 70.1 M. 38.1 M.	Surface: spalling
	16NCD13	Shaft	V1 V1 V1		3	1800 MPa	200 M. 200 M. 200 M.	n/a
	16NCD13	Shaft	V1 V1 V1		3	1500 MPa	200 M. 200 M. 200 M.	n/a
	32CDV13	Ring	DA-Version 1		3	2400 MPa	58.6 M. 40.3 M. 36.8 M.	Surface: spalling
	32CDV13	Ring	DA-Version 1		1	1800 MPa	200 M.	n/a
	32CDV13	Ring	DA-Version 1		0	1500 MPa	Canceled	n/a
	32CDV13	Shaft	V2 V2		1	2400 MPa	135.68 M.	Surface: peeling
	32CDV13	Shaft	V2 V2		2	1800 MPa	200 M. 200 M.	n/a
	32CDV13	Shaft	V2		1	1500 MPa	200 M.	n/a
Phase I.2	M50Nil	Ring	BB-Version 4	Reduced surface hardness	3	2400 MPa	88.5 M. 57.1 M. 43.0 M.	Surface: spalling
	16NCD13	Shaft	V3		3	2400 MPa	32.31 M. 55.84 M. 84.31 M.	Surface: spalling
	32CDV13	Ring	DC-Version 4		2	2400 MPa	67.7 M. 48.4 M. 54.2 M.	Surface: spalling
	32CDV13	Shaft	V4		1	2400 MPa	1.1 M. 22.7 M. 14.6 M.	Surface: peeling
Phase I.2	M50Nil	Ring	BA-Version 2	Reduced case hardening depth	3	2400 MPa	45.5 M. 108.8 M. 106.0 M.	Surface: spalling
	16NCD13	Shaft	V5		3	2400 MPa	76.70 M. 86.71 M. 52.13 M.	Surface: spalling
	32CDV13	Ring	DB-Version 2		3	2400 MPa	47.5 M. 66.5 M. 31.0 M.	Surface: spalling
	32CDV13	Shaft	V6		0	2400 MPa	14.1 M. 97 M. 9.5 M.	Surface: peeling

Phase I.2	M50Nil	Ring	BC-Version 3	Modified residual stress	3	2400 MPa	84.8 M. 43.5 M. 47.8 M.	Surface: spalling
	16NCD13	Shaft	V11		3	2400 MPa	107.8 M. 13.6 M. 67.7 M.	Surface: spalling
	32CDV13	Ring	DD-Version 3		3	2400 MPa	83.3 M. 78.3 M. 86.8 M.	Surface: spalling
	32CDV13	Shaft	V10.1		1	2400 MPa	11.5 M. 0.5 M. 41.8 M. 14.6 M	Surface: peeling
Phase II	16NCD13	Hollow shaft	V1.1	Baseline	3	2400 MPa	115.6 M. 82.9 M. 39.4 M. 32.4 M.	No spalling / no crack propagation
	16NCD13	Hollow shaft	V1.1		3	2900 MPa	9.4 M. 13.2 M. 1.2 M.	No spalling / finite crack
	32CDV13	Hollow shaft	V2.1		3	2400 MPa	35.8 M. 30.1 M. 5.4 M.	Finite crack / crack network to surface
	32CDV13	Hollow shaft	V2.1		3	2900 MPa	1.3 M. 0.6 M. 0.7 M.	Finite crack / crack network to surface
	M50Nil	Ring with notch	T104		3	2400 MPa	2.1 M. 2.9 M. 2.2 M.	Spalling with through crack
	32CDV13	Ring with notch	T104		3	2400 MPa	113.3 M. 86.6 M. 115.6 M.	Spalling / no through crack
	M50Nil	Ring with notch	T102		3	1800 MPa	n/a 200 M. 200 M.	Spall with severe cracks / No spall-reaching suspension time
	32CDV13	Ring with notch	T102 Pre-test		1	2400 MPa		Spalling with through crack
	32CDV13	Ring with notch	T102		1	1800 MPa	200 M.	No spall-reaching suspension time
	32CDV13	Ring with notch	T102		3	2400 MPa	n/a 200 M. 200 M.	Spalling without crack / No spall-reaching suspension time
Phase I.1	M50 Nil	Ring	B-Version 1 – long duration	Baseline	1	2400 MPa	43.4 M.	Surface: spalling
	32CDV13	Ring	DA-Version 1 – long duration		1	2400 MPa	54.3 M.	Surface: spalling

Table 7: Overview of tests in stream 2

				Test results variation compared to baseline		
Phase	Specimen	Material	Change compared to baseline	Max. spalling depth [mm]	Lifetime to spall initiation (mean value) [millions]	Crack
Phase I.1	V1	16NCD13	Baseline*	0.3	54	No Crack
Phase I.2	V3	16NCD13	Increased CHD	-55%*	-27%*	No Crack
Phase I.2	V5	16NCD13	Increased CHD with salt bath hardening	-47%*	-9%*	No Crack
Phase I.2	V11	16NCD13	Intermediate heating and surface rolling	-47%*	-20%*	No Crack
Phase II	V1.1	16NCD13	Hollow shaft, 2.4 GPa	No spalling	-14%*	Yes, into depth
Phase II	V1.1	16NCD13	Hollow shaft, 2.9 GPa	No spalling	-89%*	Yes into depth
*variation according to marked reference baseline (16NCD13 – V1)						

Table 8: Overview of test results for 16NCD13 shaft specimens

				Test results variation compared to baseline		
Phase	Specimen	Material	Change compared to baseline	Max. spalling depth [mm]	Lifetime to spall initiation (mean value) [millions]	Crack
Phase I.1	V2	32CDV13	Baseline**	0.096	135	No Crack
Phase I.2	V4	32CDV13	Increased NHD	+97%**	-90%**	No Crack
Phase I.2	V6	32CDV13	Nitro carburizing process	-80%**	-26%**	No Crack
Phase I.2	V10.1	32CDV13	Intermediate heating	+56%**	-82%**	No Crack
Phase II	V2.1	32CDV13	Hollow shaft, 2.4 GPa	No classical spalling	-82%**	Yes, into depth with breakouts of surface
Phase II	V2.1	32CDV13	Hollow shaft, 2.9 GPa	No classical spalling	-98%**	Yes, into depth with breakouts of surface
**variation according to marked reference baseline (32CDV13 – V1)						

Table 9: Overview of test results for 32CDV13 shaft specimens

				Test results variation compared to baseline		
Phase	Specimen	Material	Change compared to baseline	Max. spalling depth [mm]	Lifetime to spall initiation (mean value) [millions]	Crack
Phase I.1	B-Version 1	M50Nil	Baseline*	0.381	43.8	Finite crack
Phase I.2	BA-Version 2	M50Nil	Reduced hardness depth	+4%*	-27%*	Finite crack
Phase I.2	BC-Version 3	M50Nil	Increased compressive residual stress	+30%*	-53%*	Finite crack
Phase I.2	BB-Version 4	M50Nil	Reduced surface hardness and hardness depth	+29%*	-47%*	Finite crack
Phase II	B T104-Version 1	M50Nil	Notch design – less severe	+84%*	-99%*	Crack through thickness
Phase II	B T102-Version 1	M50Nil	Notch design – more severe	No general statement possible due to spread of results / inconsistency		
*variation according to marked reference baseline (M50Nil – V1)						

Table 10: Overview of test results for M50Nil outer ring specimens

				Test results variation compared to baseline		
Phase	Specimen	Material	Change compared to baseline	Max. spalling depth [mm]	Lifetime to spall initiation (mean value) [millions]	Crack
Phase I.1	DA-Version 1	32CDV13	Baseline**	0.399	114.8	Finite crack
Phase I.2	DB-Version 2	32CDV13	Reduced hardness depth	+6%**	+5%**	Finite crack
Phase I.2	DD-Version 3	32CDV13	No change (slight reduction of compressive residual stress)	+10**	+44%**	Finite crack
Phase I.2	DC-Version 4	32CDV13	Reduced surface hardness and hardness depth	+21%**	+22%**	Finite crack
Phase II	DA T104-Version 1	32CDV13	Notch design – less severe	+33%**	-12%**	Finite crack
Phase II	DA T102-Version 1	32CDV13	Notch design – more severe	No general statement possible due to spread of results / inconsistency		
**variation according to marked reference baseline (32CDV13 – V1)						

Table 11: Overview of test results for 32CDV13 outer ring specimens

European Union Aviation Safety Agency

European Union Aviation Safety Agency

Konrad-Adenauer-Ufer 3
50668 Cologne
Germany

Project website https://www.easa.europa.eu/research-projects/integrity-improvement-rotorcraft-main-gear-box-mgb

Tel. +49 221 89990- 000
Mail research@easa.europa.eu
Web www.easa.europa.eu

An Agency of the European Union